Atmos. Chem. Phys. Discuss., doi:10.5194/acp-2016-504, 2016
Manuscript under review for journal Atmos. Chem. Phys.
Published: 20 June 2016

Atmospheric Chemistry and Physics
Open Access
Discussions

Biomass Burning Aerosols and the Low Visibility Events in Southeast Asia

Hsiang-He Lee[1@], Rotem Z Bar-Or[2], and Chien Wang[1,2]

[1] Center for Environmental Sensing and Modeling, Singapore-MIT Alliance for Research and Technology, Singapore

[2] Center for Global Change Science, Massachusetts Institute of Technology, Cambridge, MA, U.S.A.

Submitted to

Atmospheric Chemistry and Physics

June 14, 2016

[@]Corresponding author address: Dr. Hsiang-He Lee, 1 Create Way, #09-03 CREATE Tower, Singapore, 138602
E-mail: hsiang-he@smart.mit.edu

Abstract

Fires including peatland burning in Southeast Asia have become a major concern of general public as well as governments in the region. This is because that aerosols emitted from such fires can cause persistent haze events under favorite weather conditions in downwind locations, degrading visibility and causing human health issues. In order to improve our understanding of the spatial-temporal coverage and influence of biomass burning aerosols in Southeast Asia, we have used surface visibility and particulate matter concentration observations, added by decadal long (2002 to 2014) simulations using the Weather Research and Forecasting (WRF) model with a fire aerosol module, driven by high-resolution biomass burning emission inventories. We find that in the past decade, fire aerosols are responsible for nearly all the events with very low visibility (< 7km), and a substantial fraction of the low visibility events (visibility < 10 km) in the major metropolitan areas of Southeast Asia: 38% in Bangkok, 35% in Kuala Lumpur, and 34% in Singapore. Biomass burnings in Mainland Southeast Asia account for the largest contributor to total fire produced $PM_{2.5}$ in Bangkok (99.1%), while biomass burning in Sumatra is the major contributor to fire produced $PM_{2.5}$ in Kuala Lumpur (49%) and Singapore (41%). To examine the general situation across the region, we have further defined and derived a new integrated metric for 50 cities of the Association of Southeast Asian Nations, i.e., Haze Exposure Days (HEDs) that measures the annual exposure days of these cities to low visibility (< 10 km) caused by particulate matter pollution. It is shown that HEDs have increased steadily in the past decade across cities with both high and low populations. Fire events are found

Atmos. Chem. Phys. Discuss., doi:10.5194/acp-2016-504, 2016
Manuscript under review for journal Atmos. Chem. Phys.
Published: 20 June 2016

to be responsible for about half of the total HEDs. Therefore, our result suggests that in order to improve the overall air quality in Southeast Asia, mitigation policies targeting at both biomass and fossil fuel burning sources need to be put in effect.

Atmos. Chem. Phys. Discuss., doi:10.5194/acp-2016-504, 2016
Manuscript under review for journal Atmos. Chem. Phys.
Published: 20 June 2016

1 Introduction

In recent decades, biomass burning has become frequent and widely spread across the mainland of Southeast Asia to the islands of Sumatra and Borneo (Langner et al., 2007; Carlson et al., 2012; Page et al., 2002; van der Werf et al., 2010). Abundant particulate matters emitted from such fires cause the haze events to occur in the downwind locations such as Singapore (Koe et al., 2001; Heil et al., 2007; See et al., 2006), degrading visibility and threatening on human health (Emmanuel, 2000; Kunii et al., 2002; Johnston et al., 2012; Mauderly and Chow, 2008). Besides causing air quality issues, fire aerosols contain rich carbonaceous compounds such as black carbon (BC) (Fujii et al., 2014) and thus can reduce sunlight through both absorption and scattering. Based on satellite data and numerical simulations, Tosca et al. (2010) found that tropospheric heating from BC absorption in the Maritime Continent (MC) is 20.5±9.3 W m^{-2}, and the reduction of both surface net shortwave radiation and regional precipitation can be as high as 10% due to the direct and semi-direct effects of fire aerosols. Nevertheless, indirect effects of fire aerosols are even more complicated due to various cloud types and meteorological conditions in the MC (Sekiguchi et al., 2003; Lin et al., 2013; Wu et al., 2013).

Majority of present day fires in Southeast Asia occurs due to human interferences: oil palm plantation related land clearing, deforestation, and peatland management, and burning of agriculture wastes (Dennis et al., 2005; Miriam et al., 2015b). Certain policies and regulations regarding, e.g., migration also affect the occurrence of burning events. For example, large fires have occurred since 1960s in

Sumatra; however, the first fire event in Kalimantan happened in the 1980s (Field et al., 2009). Based on economic incentives and population growth in Southeast Asia, future land-use management will play an important role in determining the coverage of fires across the region (Carlson et al., 2012; Miriam et al., 2015a).

Besides human interventions, meteorological factors, such as rainfall, can also influence fire initiation, intensity, and duration (Reid et al., 2012; Reid et al., 2015). Reid et al. (2012) investigated relationships between fire hotspot appearance and various climate variabilities as well as meteorological phenomena in different temporal scales over the MC, including: (1) El Nino and Southern Oscillation (ENSO) (Rasmusson and Wallace, 1983) and the Indian Ocean Dipole (IOD)(Saji et al., 1999); (2) Seasonal migration of the Inter-tropical Convergence Zone (ITCZ) and associated Southeast Asia monsoons (Chang et al., 2005); (3) Intra-seasonal variabilities such as Madden-Julian Oscillation (MJO) (Madden and Julian, 1971) and the west Sumatran low (Wu and Hsu, 2009); (4) Wave, mesoscale features, and tropical cyclones; and (5) Convections. One interesting finding is that the influence of these factors on fire events varies over different parts of the MC. For example, the fire signal in a part of Kalimantan is strongly related to both the monsoons and ENSO. In contrast, fire activity in Central Sumatra is not as closely tied to the monsoons and ENSO but MJO signal.

Above climate variabilities or meteorological phenomena affect not only biomass burning emissions but also fire aerosol transport (Reid et al., 2012). Seasonal migration of the ITCZ and associated monsoonal circulation dominate seasonal wind flows, whereas sea breeze, typhoon, or topography determine air

Atmos. Chem. Phys. Discuss., doi:10.5194/acp-2016-504, 2016
Manuscript under review for journal Atmos. Chem. Phys.
Published: 20 June 2016

flow in smaller spatial scales or shorter temporal scales, all of them play significant roles in determining the transport pathway of fire aerosols (Wang et al., 2013). For example, during the intense haze episode of June 2013, the long lasting situation with "very unhealthy" air pollution level in Singapore was actually caused by an enhanced fire aerosol transport from Sumatra to West Malaysia owing to a tropical storm located in South China Sea. Recently, using a global chemistry transport model combining with a back-trajectory tracer model, Reddington et al. (2014) attempted to attribute particulate pollutions in Singapore over a short time period of 5 years to different burning sites in surrounding regions. The coarse 2.8-degree resolution model used in the study, however, has left many open questions.

In this study, we aim to examine and quantify the impact of fire aerosols on the visibility and air quality of Southeast Asia in the past decade. Analyses of observational data and comprehensive regional model simulations have both been performed in order to improve our understanding of this issue. We firstly describe methodologies adopted in the study, followed by the results and findings from our assessment of the fire aerosol on the degradation of visibility in several selected cities and also in the great Southeast Asia. We then discuss the sensitivity of our findings to the use of different meteorological datasets as well as fire emission inventories. The last section summarizes and concludes our work.

Atmos. Chem. Phys. Discuss., doi:10.5194/acp-2016-504, 2016
Manuscript under review for journal Atmos. Chem. Phys.
Published: 20 June 2016

Atmospheric Chemistry and Physics Discussions

2 Methodology

2.1 The model

In order to address the targeted science question, we have used the Weather Research and Forecasting (WRF) model coupled with chemistry component (WRF-Chem). The WRF model is a compressible, non-hydrostatic regional meteorology model that uses the Arakawa C grid and terrain-following hydrostatic pressure coordinates, and includes various dynamic cores and physical parameterizations for different scientific purposes (Skamarock et al., 2008). The WRF-Chem model is a version of the standard WRF with an additional interactively coupled model of atmospheric chemistry. WRF-Chem simulates atmospheric evolutions of chemical species including particulate matters concurrently with meteorological fields, using the same grid structure, advection scheme, and physics schemes for sub-grid scale transport as in the standard WRF model (Grell et al., 2005). In this study, we use WRF-Chem version 3.6 with a modified chemistry tracer module instead of a full chemistry package. This is for the purpose to focus on the fire aerosol life cycle as the first step, without involving a much more complicated gaseous and aqueous chemical processing calculations. This configuration also lowers the computational burden substantially, and thus enables us to conduct long model integrations to determine the contributions of fire aerosol to the degradation of air quality in the region over the past decade. The numerical simulations are employed within a model domain with a horizontal resolution of 36 km, including 432 × 148 horizontal grid points (Fig. 1), and 31 vertically staggered layers based on a terrain-following pressure coordinate system. The vertical layers are stretched with a higher resolution near the surface (an average depth of ~30 m in the first model half layer). Variables other than vertical velocity and geopotential are stored at the half model layers. The time step is 180 seconds. The physics schemes included in the simulations are listed in Table 1. The initial and boundary meteorological conditions are taken from reanalysis meteorological dataset. In order to examine the potential influence of different reanalysis products on simulation results, we have used two such datasets: (1) the National Center for Environment Prediction FiNaL (NCEP-FNL) reanalysis data (National Centers for Environmental Prediction, 2000), which has a spatial resolution of 1 degree and a temporal resolution of 6 hours; and (2) ERA-Interim, which is a global atmospheric reanalysis from European Centre for Medium-Range Weather Forecasts (ECMWF) (European Centre for Medium-Range Weather, 2009), providing 6-hourly atmospheric fields on sixty pressure levels from surface to 0.1 hPa with a horizontal resolution of approximately 80 km. Sea surface temperature is updated every 6 hours in both NCEP-FNL and ERA-Interim. All simulations used four-dimensional data assimilation (FDDA) to nudge NCEP-FNL or ERA-Interim temperature, water vapor, and zonal and meridional wind speeds above the planetary boundary layer (PBL). This approach has shown to provide realistic temperature, moisture, and wind fields in a long simulation (Stauffer and Seaman, 1994).

In WRF-Chem, the sinks of $PM_{2.5}$ particles include dry deposition and wet scavenging calculated at every time step.

Atmos. Chem. Phys. Discuss., doi:10.5194/acp-2016-504, 2016
Manuscript under review for journal Atmos. Chem. Phys.
Published: 20 June 2016

2.2 Biomass burning emissions

Two biomass burning emission inventories are used in this study to investigate the sensitivity of modeled fire aerosol concentration to different emission estimations. The first emission inventory is the Fire INventory from NCAR version 1.5 (FINNv1.5) (Wiedinmyer et al., 2011), which classifies burnings of extra tropical forest, topical forest (including peatland), savanna, and grassland. It is used in this study to provide daily, 36 km resolution $PM_{2.5}$ emissions. The second emission inventory is the Global Fire Emission Database with version 4.1 with small fire included (GFEDv4.1s) (van der Werf et al., 2010; Randerson et al., 2012; Giglio et al., 2013). GFEDv4.1s provides $PM_{2.5}$ emissions with the same spatiotemporal resolution as FINNv1.5.

A plume rise algorithm for fire emissions was implemented in WRF-Chem by Grell et al. (2011) to estimate fire injection height. This algorithm, however, often derives an injection height for tropical peat fire that is too high comparing to the estimated value based on remote sensing retrievals (Tosca et al., 2011). Therefore, we have limited the plume injection height of peat fire within 700 m in this study based on Tosca et al. (2011). This modification has clearly improved the modeled surface $PM_{2.5}$ concentration comparing to observations in Singapore.

In order to distinguish the spatial-temporal coverage and influence of biomass burning aerosols from different regions in Southeast Asia and nearby northern Australia, we have created five tracers to represent fire aerosols respectively from Mainland Southeast Asia (s1), Sumatra and Java islands (s2), Borneo (s3), the rest of the Maritime Continent (s4), and northern Australia (s5) as illustrated in Fig. 1. The

Atmos. Chem. Phys. Discuss., doi:10.5194/acp-2016-504, 2016
Manuscript under review for journal Atmos. Chem. Phys.
Published: 20 June 2016

major fire season in Mainland Southeast Asia (s1) is from February to April. In other four regions (s2-s5), it is from August to October.

Generally speaking, there are strong seasonal variations of fire emissions coordinating with those of rainfall in all fire regions as shown in Fig. 2. Because Mainland Southeast Asia (s1) and northern Australia (s5) are on the edge of seasonal migration of the ITCZ, seasonal variations of rainfall in these two regions are even more pronounced. Sumatra (s2), Borneo (s3), and the rest of the Maritime Continent (s4) are all influenced by similar meteorological regimes, i.e., seasonal migration of the ITCZ. However, the passage of MJO events adds more intra-season variability of rainfall and fire emissions in these three regions. Therefore, the seasonal variations of rainfall and fire emissions in s2, s3, and s4 are not as apparent as in the s1 and s5 regions (Fig. 2b – d), owing to the influences of multiple scales of precipitation features over these areas. Nevertheless, inter-seasonal variations of rainfall and fire emissions are still highly correlated with each other in these three regions (see additional discussion in Section 4).

2.3 Observational data and model derivation of visibility

The definition of "visibility" is the farthest distance at which one can see a large, black object against a bright background at the horizon (Seinfeld and Pandis, 2006). There are several factors to determine visibility, but in this study we mainly consider the absorption and scattering of light by gases and particles excluding fog or misty days. One of the most widely used equations, *Koschmeider equation*, is given by

$$VIS = 3.912 / b_{ext}, \quad (1)$$

where *VIS* is visibility with a unit in meter and b_{ext} is the extinction coefficient with a unit of m^{-1}. Visibility degradation is most readily observed from the impact of particulate pollution besides fog. Based on Eq. (1), a maximum visibility under absolutely dry and pollution-free air is about 296 km owing to Rayleigh scattering, while a visibility on the order of 10 km is considered as a moderately to heavily polluted air by particulate matters. Abnormal and persistent low visibility situations are also referred to as "haze" events. Urban air pollutions such as fossil fuel burning can cause low visibility and haze event to occur. Similarly, fire aerosols, alone or mixed with other particulate pollutants, can degrade visibility and lead to haze events too.

The observational data of visibility from the Global Surface Summary of the Day (GSOD) (Smith et al., 2011) are used in our study, as derived from the Integrated Surface Hourly (ISH) dataset and archived at the National Climatic Data Center (NCDC). The daily visibility in the dataset is available from 1973 to present.

In order to compare with observations, we also calculate the visibility using modeled fire aerosol data, based on the extinction coefficient of these aerosols as functions of particle size (assuming a log-normal size distribution of accumulation mode, with a standard deviation $\sigma = 2$), the complex refractive index of the particles, and a wavelength of 550 nm of the incident light. As fire plumes contain both sulfur compounds and carbonaceous aerosols, we assume the fire aerosols are aged internal mixtures with black carbon as core and sulfate as shell (Kim et al., 2008). We also consider hydroscopic growth of sulfate fraction of these mixed particles in the calculation based on environmental relative humidity.

Atmos. Chem. Phys. Discuss., doi:10.5194/acp-2016-504, 2016
Manuscript under review for journal Atmos. Chem. Phys.
Published: 20 June 2016

Atmospheric Chemistry and Physics Discussions

As mentioned above, a visibility of 10 km is considered as under moderately to heavily particulate pollution so that this quantity is used as the threshold for deriving the "low visibility day (VLD)" in our study. In analysis, we derived firstly the low visibility days in every year for a given city using the GSOD visibility data. Such day is identified when the daily averaged visibility in the observation site is lower or equal to 10 km. Then, we derived the low visibility days in the same procedure, but using modeled visibility data that were only influenced by fire aerosols. Both the observed and modeled visibilities were then used to define the fraction of low visibility days caused by fire aerosols. It is assumed that whenever fire aerosol alone could cause a low visibility day to occur, such a day would be attributed to fire aerosol caused LVD, regardless whether other coexisting pollutants would have an intensity to cause low visibility or not. We have also used a daily visibility of 7 km as the criterion to define the "very low visibility day (VLVD)". Such heavy haze events in the region are generally caused by severe fire aerosol pollution, thus we use their occurrence specifically to evaluate the model performance.

2.4 Numerical simulations

Our simulations cover a time period slightly longer than a decade from 2002 to 2014 based on availability of biomass burning emission estimations. The simulation of each year started on 1 November of the previous year and lasted for 14 months. The first two months are used for spin-up.

Three sets of decadal long simulations have been conducted. The first simulation used reanalysis data of NCEP-FNL and fire emission inventory of

FINNv1.5. This simulation is hereafter referred to as FNL_FINN and discussed as the base simulation. In order to examine the influence of different meteorological inputs on fire aerosol life cycle, the second simulation was conducted using the same FINNv1.5 fire emission inventory as in FNL_FINN but a different reanalysis data of ERA_Interim, referring to as ERA_FINN. In addition, to investigate the variability of fire aerosol concentration brought by the use of different estimations of fire emissions, the third simulation, FNL_GFED, was driven by the same NCEP-FNL meteorological input as in FNL_FINN but a different fire emission inventory, the widely used GFEDv4.1s. Since the daily emission of GFEDv4.1s is only available after 2003, the period of the FNL_GFED simulation is from 2003 to 2014.

Precipitation is one of the key factors in determining the transport and scavenging of fire aerosols. WRF simulation driven by NCAR_FNL reanalysis data, or the FNL_FINN run, produced a monthly mean precipitation of 6.81±0.55 mm day^{-1} over the modeled domain for the period from 2002 to 2014, very close to the value of 6.29±0.43 mm day^{-1} produced in another simulation driven by ERA_Interim, or the ERA_FINN run. Comparing to the monthly mean of 4.69±0.38 mm day^{-1} from the satellite retrieved precipitation in the Tropical Rainfall Measuring Mission (TRMM) 3B43 (V7) dataset (Huffman et al., 2007), however, both results appear to be higher. Based on the sensitivity tests for FDDA grid nudging, the wet bias in both experiments mainly comes from water vapor nudging. Figure 3a – c are the Hovmöller plot of daily TRMM, FNL_FINN, and ERA_FINN precipitation in 2006, respectively. Comparing to the observations, both FNL_FINN and ERA_FINN have produced more light rain events, and this appears to be the reason behind the model

Atmos. Chem. Phys. Discuss., doi:10.5194/acp-2016-504, 2016
Manuscript under review for journal Atmos. Chem. Phys.
Published: 20 June 2016

precipitation bias. Despite the model overestimation in averaged total precipitation, the temporal correlation of normalized rainfall anomaly between FNL_FINN (ERA_FINN) and TRMM is 0.69 (0.90) and the spatial correlation is 0.86 (0.85) during 2002-2014. The comparisons show that simulated rainfall generally agrees with the observation in space and time, especial when ERA-Interim reanalysis is used (i.e., in ERA_FINN).

3 Assessment of the impact of fire aerosols on Southeast Asia visibility

3.1 Impact of fire aerosols on the visibility in four selected cities

We first to focus our analysis on four selected cities in the region, Bangkok (Thailand), Kuala Lumpur (Malaysia), Singapore (Singapore), and Kuching (Malaysia), all located close to the major Southeast fire sites ranging from the mainland to the islands. Specifically, Bangkok is a smoke receptor city of the fire events in the mainland of Southeast Asia (s1) while Kuala Lumpur and Singapore are two cities frequently under the influence of Sumatra (s2) as well as Borneo fires (s3). Kuching is in the coast area of Borneo so that directly affected by Borneo fire events (s3).

The low visibility events in these four near-fire-site cities during the fire seasons from 2002 to 2014, defined as days with daily averaged visibility lower or equal to 10 km, or Low Visibility Days (LVDs), have been identified using the daily GSOD visibility database and then compared with modeled results (Fig. 4). We find that the model has reasonably captured the LVDs despite certain biases. Specifically, for the Very Lower Visibility Days (VLVDs), here defined as events with daily averaged visibility lower or equal to 7 km, the modeled and observed results display a good correlation despite a model overestimate in visibility value or underestimate in degrading visibility in certain events. In Southeast Asia, severe haze events equivalent to the VLVDs in visibility degradation are largely caused by fire aerosol pollutions. Assuming this is true, the performance of our model in reproducing the major fire events is very good since only 10% or fewer VLVDs observed in the past decade were not captured by the model (Table 2; Fig. 4). Note that other than these VLVDs, for many LVDs fire aerosol might not be the only reason responsible for the degradation of visibility.

In addition to the visibility data, we have also obtained the ground-based observations of $PM_{2.5}$ concentration in recent years from the National Environment Agency (NEA) of Singapore. Figure 5a shows the comparison of time series of observed and FNL_FINN simulated daily $PM_{2.5}$ during 2013-2014. Note that the observed $PM_{2.5}$ level reflects the influences of both fire and non-fire aerosols, whereas the modeled $PM_{2.5}$ only includes the impact of fire aerosols. However, model still predicted clearly high $PM_{2.5}$ concentrations during most of the observed haze events, especially in June 2013 and in spring and fall seasons of 2014 (highlighted green areas), though with underestimates in particle concentration of up to 30-50%, likely due to the model resolution, a model overestimation of rainfall, and the errors in emission inventory. Once again, the model has shown a solid performance in capturing all the major known haze events caused by fire PM in Singapore (Fig. 5b). Specifically to the observed VLVDs, we evidence that fire aerosol is the main reason behind these events.

We find that the annual mean LVDs in Bangkok has increased from 46% in the first 5-year period of the simulation duration (2002-2009) to 74% in the last 5-year period (2010-2014), so does the LVDs caused by fire aerosols (Fig. 6a). Overall, fire aerosols are responsible for more than one third of these LVDs (i.e. 38% in average; Table 2). The largest source of fire aerosols affecting Bangkok is agriculture waste and other biomass burning in s1 during the dry season of spring (Fig. 7a; Table 3). During the fire season, abundant fire aerosols degrade visibility and even cause VLVDs to occur (Fig. 6e). Ninety-eight percent of VLVDs in Bangkok occurred from December to April. Based on our model results, 89% of VLVDs can be identified as fire caused.

In Kuala Lumpur, the percentage of LVDs also gradually increases since 2006 to reach a peak in 2011 and again in 2014 (Fig. 6b). During 2005-2010 the frequency of total LVDs have increased 10-15% each year, mainly attributing to the pollution sources other than fires. However, fire-caused LVDs are more evident after 2009. Seasonal wise, there are two peaks of fire aerosol influence, one in February-March and another in August (Fig. 6f), corresponding to the trans-boundary transport of fire aerosols from Mainland Southeast Asia (s1) in the winter monsoon season and from Sumatra (s2) in the summer monsoon season, respectively (Fig. 7b). Three quarter of VLVDs are occurred in the summer monsoon season due to Sumatra fires. Noted that in November and December the percentage of LVDs is over 50% and dominated by the pollutants other than fire aerosols. These non-fire aerosols come from either local sources or the areas further inland riding on the winter monsoon

Atmos. Chem. Phys. Discuss., doi:10.5194/acp-2016-504, 2016
Manuscript under review for journal Atmos. Chem. Phys.
Published: 20 June 2016

circulation. Overall, fire pollution is responsible for 35% or a substantial fraction of total low visibility events in Kuala Lumpur during 2002-2014 (Table 2).

The percentage of LVDs in Singapore has been rapidly increasing since 2012 (Fig. 6c). Except for 2014, this increase is mostly from anthropogenic pollution other than fires, especially in 2012 and 2013. High percentage of LVDs in November and December could be induced by aerosols from further inland of Mainland Southeast Asia through long-range transport driven by the monsoon circulation (Fig. 6g). Similar to Kuala Lumpur, there are two peaks of fire aerosol influence, one in February-March and another in September-October (Fig. 6g). The trans-boundary transported fire aerosols can come from both Sumatra (s2) and Borneo (s3) in the summer monsoon season (Fig. 7c). Except for the severe haze events in June 2013, VLVDs basically occur in September and October (i.e. 92%) due to both Sumatra and Borneo fires. In general, 34% of LVDs in Singapore are caused by fire aerosols in the FNL_FINN simulation and the rest by local and long-range transported pollutants (Table 2). Fire aerosol is still the major reason for the episodic severe haze conditions.

Because of its geographic location, Kuching is affected heavily by local fire events during the fire season (Fig. 7d). Fire aerosols can often degrade the visibility easily to lower than 7 km and even reach 2 km (Fig. 4d). The LVDs mainly occur in August and September during the fire season (Fig. 6d and h). The frequency of LVDs in Kuching is similar to Singapore; however, 25% of those LVDs are considered to be VLVDs in Kuching while only 4% are in Singapore in comparison (Table 2).

Atmos. Chem. Phys. Discuss., doi:10.5194/acp-2016-504, 2016
Manuscript under review for journal Atmos. Chem. Phys.
Published: 20 June 2016

3.2 Impact of fire aerosols on the visibility in the greater Southeast Asia

Air quality degradation caused by fires apparently occurs in regions beyond the above-analyzed four cities. To examine such degradation in the greater Southeast Asia, we have extended our analysis to cover 50 cities of the Association of Southeast Asian Nations (ASEAN). The impact of particulate pollution on the greater Southeast Asia is measured by a metric of "Haze Exposure Day" (HED). HED can be defined in a population weighted format for the 50 analyzed cities, indicating the relative exposure of the populations in these cities to the low visibility events caused by particulate pollution, thus calculated as:

$$HED_{pw} = \sum_{i=1}^{N} C_{pw}(i), \quad (2)$$

here,

$$C_{pw}(i) = pop(i) \cdot C(i) / \sum_{i=1}^{N} pop(i), \quad (3)$$

where N equals to the total number of cities, or 50, i is the index for the 50 analyzed cities, $C_{pw}(i)$ is the population-weighted fraction of the total Haze Exposure Days and *pop(i)* is the population for a given city, *C(i)* represents the annual LVDs for that city calculated from the GSOD dataset. Note that we assume that the population of each city is constant throughout the analyzed period. Another assumption of HED_{pw} is that everyone in a given city would equally expose to the particulate pollution. The top four among the 50 cities that made the largest contributions to the HED_{pw} are Jakarta, Bangkok, Hanoi, and Yangon, with population ranking of 1, 2, 4, and 5, respectively (Fig. 8a).

Atmos. Chem. Phys. Discuss., doi:10.5194/acp-2016-504, 2016
Manuscript under review for journal Atmos. Chem. Phys.
Published: 20 June 2016

Atmospheric Chemistry and Physics Discussions

In addition, HED can be also defined in an arithmetic mean format, assuming each city weights equally regardless of its population. Its value hence emphasizes on the relative exposure of each area within the analyzed region:

$$HED_{ar} = \sum_{i=1}^{N} C(i)/N, \qquad (4)$$

Apparently, both HED_{pw} and HED_{ar} can be also calculated using fire-caused LVDs (here using the results of FNL_FINN) to define the absolute and relative contributions of fire aerosols to the total low visibility events in the region. We will label the fire-caused HED as $fHED_{pw}$ and $fHED_{ar}$ thereafter.

We find that both HED_{pw} and HED_{ar} increase rather steadily over the past decade (Fig. 8b), demonstrating that the exposure to haze events either weighted by population or not has become worse in the region. Generally speaking, the fire aerosols are responsible for 40-60% of the total exposures to low visibility across the region. In both measures, the increase of fire-caused HED (2.64 and 3.37 days per year for population-weighted and arithmetic mean, respectively) is similar to that of overall HED (2.61 and 3.59 days per year for population-weighted and arithmetic mean, respectively) (Fig. 8b), suggesting that fire aerosol has taken the major role in causing the degradation of air quality in Southeast Asia comparing to the non-fire particulate pollution. The result that HED_{pw} is higher than HED_{ar} in most of the years indicates that the particulate pollution is on average worse over more populous cities than the others. Interestingly, the discrepancy of these two variables, however, has become smaller in recent years and even reversed in 2014, implying an equally worsening of haze event occurrence across from the smaller to the bigger cities in terms of population in the region. The reason behind this result could be a widely spread of fire events in the region, particularly causing acute haze events in the cities with relatively low populations. Regarding the increase of fire-caused HED, because biomass burning, especially peatland burning usually occurs in the rural areas, higher fire emissions would extend low visibility condition to a larger area regardless of its population. On the other hand, air pollution caused by industrialization, urbanization, and other factors such as population growth increases rapidly across the region so that even cities with lower population now increasingly suffer from low visibility from fossil fuel burning and other sources of particulate pollution. Therefore, the mitigation of air quality degradation needs to consider both fire and non-fire sources.

3.3 The influence of wind and precipitation on fire aerosol life cycle

Seasonal migrations of the ITCZ and associated summer and winter monsoons dominate seasonal wind flows that drive fire aerosol transport. Additionally, as discussed previously, certain small scale or short-term phenomena such as sea breeze, typhoon, and topography forced circulations also play important roles in distributing fire aerosols. Nevertheless, we focus our discussions here on the former.

February to April is the main fire season in Mainland Southeast Asia (s1). In the FNL_FINN simulation, seasonal mean concentration of $PM_{2.5}$ within the planetary boundary layer (PBL) can exceed 20 μg m^{-3} in this region. During this fire season, the most common wind direction is from northeast to southwest across the region (Fig. 9a). Fire aerosol plumes with concentration higher than 0.1 μg m^{-3} can transport with the main wind westward as far as 7000 km from the burning sites.

Atmos. Chem. Phys. Discuss., doi:10.5194/acp-2016-504, 2016
Manuscript under review for journal Atmos. Chem. Phys.
Published: 20 June 2016

In contrast, February to April is not the typical burning season in the islands. Low fire emissions added by a lack of long-range transport of fire aerosols from the mainland due to the seasonal circulation result in a low $PM_{2.5}$ level over these regions (Fig. 9b - d).

Wet scavenging is a major factor to determine the lifetime and thus abundance of suspended fire aerosols in the air. The effect of wet scavenging of fire aerosols is reflected from the wet scavenging time calculated using the modeled results. The wet scavenging time is a ratio of aerosol mass concentration and scavenging rate, the latter is a function of precipitation rate. Thus, short scavenging time often indicates high scavenging rate except for the sites with extremely low aerosol concentration. During February-April, at the ITCZ's furthest southern extent, the short scavenging time < 1 day around 10°S shows a quick removal of fire aerosols by heavy precipitation that has prevented the southward transport of aerosols (Fig. 9f). Whereas, the long scavenging time (> 5 days) in the Western Pacific warm pool, South China Sea, the Indochina peninsula, Bay of Bengal, and Arabian Sea leads to a long suspending time of aerosols transported to these regions. During the same season, over the islands of Sumatra and Borneo, the abundance along with the likelihood of being transported to other places of fire aerosols, either emitted locally or trans-boundary transported, are greatly limited by the high scavenging rate (short scavenging time) over this regions (Fig. 9g and h). South China Sea is in a dry condition during this time period, therefore, fire aerosols from the northern part of Philippine can be transported to this region and stay longer than 5 days (Fig. 9i).

Atmos. Chem. Phys. Discuss., doi:10.5194/acp-2016-504, 2016
Manuscript under review for journal Atmos. Chem. Phys.
Published: 20 June 2016

The months of August to October, when the ITCZ reaches its furthest northern extent, mark the major fire season of Sumatra, Borneo and some other islands in the Maritime Continent (Fig. 10b - d). Australia fires also mainly occur in this season (Fig. 10e). Mean wind flows are from southeast to northwest in the Southern Hemisphere, and turn to the northeast direction once pass the Equator. Within the MC the seasonal variation of rainfall is small during this time, heavy precipitation and thus short scavenging time (< 3 days) mostly exist along the MJO path (Fig. 10f - i) (Wu and Hsu, 2009). The high scavenging rate in the regions close to the fire sites in the islands shortens the transport distance of fire aerosol plumes with $PM_{2.5}$ concentration > 0.1 μg m^{-3} to less than 3000 km (Fig. 10b - d). Long scavenging time (> 5 days) primarily exists in Banda Sea and northern Australia due to the ITCZ location. Fire aerosols from Java Island (s2) (Fig. 10g), Papua New Guinea (s4) (Fig. 10i), and northern Australia (s5) (Fig. 10j) can thus suspend in the air for a relatively long time over these regions.

The above-discussed seasonal features of precipitation and aerosol scavenging strength help us to better understand the variability of haze occurrence and also to identify the major source regions of fire aerosols influencing selected Southeast Asian cities (Fig. 7). For example, the geographic location of Bangkok, which is inside the s1 emission region, determines that about 99% fire aerosols is from sources within the region from December to April (Fig. 7a and Table 3). Fire aerosols from all the other burning sites stay at very low level even during the burning seasons there due to circulation and precipitation scavenging. For Kuala Lumpur and Singapore, over 90% of total fire aerosols reached both cities come from Mainland Southeast Asia (s1) in January–April due to the dominant winter monsoon circulation. During May-October, however, the major sources of fire aerosols shift to Sumatra (s2) and Borneo (s3) aiding by northward wind (Fig. 10b and c). The monthly variations of $PM_{2.5}$ concentration in Kuala Lumpur and Singapore also have a largely similar pattern (Fig. 8b and d). The annual mean contribution of different emission regions in Kuala Lumpur are 43% from Mainland Southeast Asia (s1), 49% from Sumatra (s2), 4% from Borneo (s3), 3% from the rest of Maritime Continent (s4), and 0.4% from northern Australia (s5) in FINL_FINN (Table 3). Similar to Kuala Lumpur, there are two peak seasons of the monthly low visibility days contributed by fire aerosols in Singapore (Fig. 6g), well correlated with modeled high fire $PM_{2.5}$ concentration (Fig. 7c). The low visibility days in March and April mainly are caused by fire aerosols from Mainland Southeast Asia (s1) under southward wind pattern (Fig. 9a), and those in May to October are affected by Sumatra (s2) first in May to June, and then by both s2 and s3 (Borneo) during August to October due to north- or northwest-ward monsoonal circulation (Fig. 10b and c; also Table 3). Kuching, similar to Bangkok, is strongly affected by local fire aerosols (s3) during fire season (July – October). The annual mean contribution from Borneo (s3) is 85% while only 7% from Mainland Southeast Asia (s1) and 5% from Sumatra (s2) (Table 3).

Reddington et al. (2014) applied two different models, a 3D global chemical transport model and a Lagrangian atmospheric transport model to examine the long-term mean contributions of fire emissions to $PM_{2.5}$ from different regions in Southeast Asia. The contribution from Mainland Southeast Asia to the above-discussed four selected cities was lower than our result during January-May, likely due to their use of a different emission inventory and the coarse resolution of their global model. FINNv1.5 dataset used in our study specifically provides higher $PM_{2.5}$ emissions from agriculture fires (the major fire type in Mainland Southeast Asia) than GFED4.1s does, the latter is an updated version the dataset (GFEDv3) used in Reddington et al. (2014) (Fig. 2). The detail comparison of FNL_FINN and FNL_GFED will be discussed in the following section.

4 Influence of different reanalysis datasets and emission inventories on modeled fire aerosol abundance

As discussed in the previous section, meteorological conditions, particularly wind field and precipitation, could substantially influence the life cycle and transport path of fire aerosols during the fire reasons; therefore, it is necessary to examine any potential discrepancies in modeled particulate matter abundance attributing to the use of different meteorological datasets.

In comparing the two of our simulations, one was driven by the NCAR_FNL (i.e., FNL_FINN), another by the ERA_Interim (i.e., ERA_FINN) meteorological input, we find that the ERA_FINN run consistently produces less precipitation than FNL_FINN run during the raining seasons over past decade (Fig. 2) (also see the comparison results of both runs with observations in Section 2.4). Regarding fire aerosol life cycle, less rainfall in ERA_FINN results in a weaker wet scavenging condition and thus higher abundance of fire aerosol concentration than in FNL_FINN. We find that annual mean concentration of fire $PM_{2.5}$ produced in the ERA_FINN run in Bangkok,

Atmos. Chem. Phys. Discuss., doi:10.5194/acp-2016-504, 2016
Manuscript under review for journal Atmos. Chem. Phys.
Published: 20 June 2016

Kuala Lumpur, Singapore, and Kuching is 8.8, 5.4, 3.4, and 7.9 μg m^{-3}, respectively, clearly higher than the corresponding results of the FNL_FINN run of 8.0, 4.9, 3.0, and 7.1 μg m^{-3} (Table 3). In Mainland Southeast Asia, a twenty-one percent lower rainfall in ERA_FINN causes the significantly different $PM_{2.5}$ concentration comparing to FNL_FINN result in the fire season (February – April) (Fig. 2a and 11a). In Kuala Lumpur, the difference in fire $PM_{2.5}$ concentration between these two runs mainly comes from Sumatra (s2) during June to September; however, in Singapore and Kuching the concentration difference comes from both Sumatra (s2) and Borneo (s3) in August to October (Fig. 11b - d and Table 3), all corresponding to the discrepancy of rainfall between FNL_FINN and ERA_FINN in these regions (Fig. 2b and c).

The difference in aerosol scavenging between ERA_FINN and FNL_FINN extends to a difference as high as 7% and 12% in the resulted LVDs of Bangkok and Kuching, respectively, (Table 2), though its influence on the results of Kuala Lumpur and Singapore is much smaller (3~4%). In general, fire $PM_{2.5}$ concentration in ERA_FINN is about 10% higher than in FNL_FINN; however, the substantial impact of fire aerosols on LVDs is more sensitive in places near the burning areas, i.e., Bangkok and Kuching. Interestingly, a mild increase of VLVDs in the ERA_FINN run in Bangkok and Kuching (~1%) (Table 2) implies that the occurrence of severe haze events is less affected by the rainfall difference in the burning areas.

In addition to meteorological inputs, differences various fire emission estimations could also affect the modeled results. To examine such an influence, we have compared two simulations with the same meteorological input but different fire emission inventories, the FNL_FINN using FINNv1.5 and FNL_GFED using GFEDv4.1s. The main differences between the two emission inventories appear mostly in Mainland Southeast Asia (s1) and northern Australia (s5) (Fig. 2a and e; Fig. 12a and e). For instance, the peak month of fire $PM_{2.5}$ concentration in Bangkok shifts from March in FNL_FINN to January in FNL_GFED (Fig. 11a), owing to the difference in temporal pattern between the two fire emission inventories (Fig. 2a). Comparing to FINNv1.5, fire emissions in GFEDv4.1s over Mainland Southeast Asia are more than 66% lower (Fig. 2a), and this results in a 40% lower fire $PM_{2.5}$ in Bangkok (Fig. 11a and Table 3). The lower fire $PM_{2.5}$ concentration in FNL_GFED actually produced a visibility that matches better with observation in Bangkok comparing to the result of FNL_FINN (Fig. S1a).

The difference in monthly fire emissions over the islands between the two emission inventories is small, with the fire emission in FINNv1.5 generally higher than that in GFEDv4.1s (Fig. 2b – d). However, fire emissions in GFEDv4.1s are much higher during the fire season in the dry years (i.e. 2004, 2006 and 2009) over s2 and s3 (Fig. 12b and c), leading to a modeled mean $PM_{2.5}$ concentration by FNL_GFED in Kuala Lumpur and Singapore that is higher than that by FNL_FINN during the fire season (Fig. 11b and c). On the other hand, the higher $PM_{2.5}$ concentration simulated in FNL_GFED during the June 2013 severe haze event in Kuala Lumpur and Singapore is due to the spatiotemporal distribution of fire spots rather than absolute fire aerosol emissions. Based on our simulations, fire aerosols from Sumatra (s2) are mainly responsible for the severe haze event in June 2013 (Fig. 7b – c and Fig. S2b – c). During this event, the total amount of fire emissions in

Sumatra (s2) is lower in GFEDv4.1s than FINNv1.5, however, distributed rather more densely over a smaller area (Fig. 13c and d). As a result, under the same meteorological condition, the simulated $PM_{2.5}$ in the FNL_GFED simulation reaches Singapore in a higher concentration that also matches better with observation than the result of FNL_FINN (Fig. 13b). A similar result also appears in Kuching, where the difference in modeled $PM_{2.5}$ concentration between the two model runs is likely related to the difference in spatial or temporal distributions rather than the mean quantities of $PM_{2.5}$ emissions since the latter are almost the same in both fire emissions inventories.

The most evident difference between the two emission inventories occurs in northern Australia, where FINNv1.5 suggests an almost negligible fire aerosol emission comparing to GFEDv4.1s (Fig. 2e). Therefore, in the FNL_GFED simulation, Australia fire aerosols play an important role in Singapore air quality, contributing to about 22% modeled $PM_{2.5}$ concentration in Singapore. In contrast, Australia fires have nearly no effect on Singapore air quality in the FNL_FINN run (Table 3). Our results raise the important issue of the sensitivity of modeled aerosol concentration in downwind areas to the spatiotemporal distribution, besides the absolute emission amount from the fire spots. A further study regarding this topic would be much needed.

5 Summary and Conclusions

We have examined the extent of the biomass burning aerosol's impact on the air quality of Southeast Asia in the past decade using visibility and surface $PM_{2.5}$

Atmos. Chem. Phys. Discuss., doi:10.5194/acp-2016-504, 2016
Manuscript under review for journal Atmos. Chem. Phys.
Published: 20 June 2016

Atmospheric Chemistry and Physics Discussions

measurements along with the WRF model with a modified fire tracer module. The model has shown a good performance in capturing 90% of the observed severe haze events (visibility < 7 km) occurred in past decade in several cities close to the major burning sites. Such events are known to be induced mainly by biomass burning. On the more general cases of particulate pollution, our study suggests that fire aerosols are responsible for a substantial fraction of the low visibility days (visibility < 10 km) in several cities: 38% in Bangkok, 35% in Kuala Lumpur, 34% in Singapore, and 32% in Kuching.

The life cycle and transport path, and thus spatial and temporal distributions of fire aerosols are all influenced by meteorological conditions, especially the seasonal precipitation distribution and atmospheric circulations. These impacts are well reflected from the variations of abundance of fire aerosols in the selected cities in analysis. In general, Mainland Southeast Asia is the major contributor during the Northeast or winter monsoon season in Southeast Asia. In the Southwest or summer monsoon season, most fire aerosols come from Sumatra and Borneo. Specifically, fires in Mainland Southeast Asia are accounted for the largest percentage of the total fire $PM_{2.5}$ in Bangkok (99.2%), and fires from Sumatra are the major contributor in Kuala Lumpur (51%) and Singapore (42%). Kuching receives 88% of fire aerosols from local Borneo fires.

By comparing the results from two modeled runs with the same fire emissions but driven by different meteorological inputs, we have examined the potential sensitivity of modeled results to meteorological datasets. The discrepancy in modeling the low visibility events due to different meteorological datasets is clearly evident, especially in the results of Bangkok and Kuching. However, using different meteorological input datasets does not appear to have influenced the modeled very low visibility events, or the severe haze events in the cities close to burning sites.

We have also examined the sensitivity of modeled results to the use of different emission inventories. We find that significant discrepancies of fire emissions in Mainland Southeast Asia and northern Australia between two emission inventories used in the study have caused significant difference in modeled fire aerosol concentration and visibility, particularly in Bangkok and Singapore. For instance, the contribution to fire aerosol in Singapore from northern Australia changes from nearly zero in the simulation driven by FINNv1.5 to about 22% in another simulation driven by GFEDv4.1s. We have also identified the influence of the discrepancy in spatiotemporal distribution rather than total emitted quantities from the fire hotspots on modeled $PM_{2.5}$ concentration. Further analysis on this direction is much needed.

To further assess the impacts of fire events on the air quality of the great Southeast Asia, we have defined and derived a metric of "Haze Exposure Days" (HEDs), by integrating annual low visibility days of 50 cities of the Association of Southeast Asian Nations and weighted by population or averaged arithmetically. We find that a very large population of Southeast Asia has been exposed to relatively persistent hazy condition. The top four cities in the HED ranking, Jakarta, Bangkok, Hanoi, and Yangon, with a total population exceeding two millions, have experienced more than 200 days per year of low visibility due to particulate pollution over the past decade. Even worse is that the number of annual low visibility days have been increasing steadily not only in high population cities but also those with relatively low populations, suggesting a widely spread of particulate pollutions into the great Southeast Asian region. Generally speaking, the fire aerosols are found to be responsible for about half of the total exposes to low visibility across the region. Our result suggests that in order to improve the air quality in Southeast Asia, besides reducing or even prohibiting planned or unplanned fires, mitigation policies targeting at pollution sources other than fires need to be put in effect as well.

Acknowledgements.

This research was supported by the National Research Foundation Singapore through the Singapore-MIT Alliance for Research and Technology, the interdisciplinary research program of Center for Environmental Sensing and Modeling. It was also supported by the U.S. National Science Foundation (AGS-1339264), U.S. DOE (DE-FG02-94ER61937) and U.S. EPA (XA-83600001-1). The authors would like to acknowledge the National Environment Agency (NEA) of Singapore for making Singapore $PM_{2.5}$ data available, the NCEP-FNL, ECMWF ERA-Interim, NCAR FINN, and GFED working groups for releasing their data to the research communities, and the NCAR WRF developing team for providing the numerical model for this study. We thank the National Supercomputing Centre of Singapore (NSCC) for providing computing resources and technical support.

Reference

Carlson, K. M., Curran, L. M., Ratnasari, D., Pittman, A. M., Soares-Filho, B. S., Asner, G. P., Trigg, S. N., Gaveau, D. A., Lawrence, D., and Rodrigues, H. O.: Committed carbon emissions, deforestation, and community land conversion from oil palm plantation expansion in West Kalimantan, Indonesia, Proceedings of the National Academy of Sciences, 109, 7559-7564, 10.1073/pnas.1200452109, 2012.

Chang, C. P., Wang, Z., McBride, J., and Liu, C.-H.: Annual Cycle of Southeast Asia—Maritime Continent Rainfall and the Asymmetric Monsoon Transition, Journal of Climate, 18, 287-301, 10.1175/JCLI-3257.1, 2005.

Dennis, R., Mayer, J., Applegate, G., Chokkalingam, U., Colfer, C. P., Kurniawan, I., Lachowski, H., Maus, P., Permana, R., Ruchiat, Y., Stolle, F., Suyanto, and Tomich, T.: Fire, People and Pixels: Linking Social Science and Remote Sensing to Understand Underlying Causes and Impacts of Fires in Indonesia, Hum Ecol, 33, 465-504, 10.1007/s10745-005-5156-z, 2005.

Emmanuel, S. C.: Impact to lung health of haze from forest fires: The Singapore experience, Respirology, 5, 175-182, 10.1046/j.1440-1843.2000.00247.x, 2000.

Field, R. D., van der Werf, G. R., and Shen, S. S. P.: Human amplification of drought-induced biomass burning in Indonesia since 1960, Nature Geosci, 2, 185-188, 2009.

Fujii, Y., Iriana, W., Oda, M., Puriwigati, A., Tohno, S., Lestari, P., Mizohata, A., and Huboyo, H. S.: Characteristics of carbonaceous aerosols emitted from peatland fire in Riau, Sumatra, Indonesia, Atmospheric Environment, 87, 164-169,2014.

Giglio, L., Randerson, J. T., and van der Werf, G. R.: Analysis of daily, monthly, and annual burned area using the fourth-generation global fire emissions database

(GFED4), Journal of Geophysical Research: Biogeosciences, 118, 317-328, 10.1002/jgrg.20042, 2013.

Grell, G., Freitas, S. R., Stuefer, M., and Fast, J.: Inclusion of biomass burning in WRF-Chem: impact of wildfires on weather forecasts, Atmos. Chem. Phys., 11, 5289-5303, 10.5194/acp-11-5289-2011, 2011.

Grell, G. A., A. Mangold, M. K., O. Mohler, H. Saathoff, H. Teichert, V. Ebert, Peckham, S. E., Schmitz, R., McKeen, S. A., Frost, G., Skamarock, W. C., and Eder, B.: Fully coupled "online" chemistry within the WRF model, Atmospheric Environment, 39, 6957-6975, 2005.

Heil, A., Langmann, B., and Aldrian, E.: Indonesian peat and vegetation fire emissions: Study on factors influencing large-scale smoke haze pollution using a regional atmospheric chemistry model, Mitig Adapt Strat Glob Change, 12, 113-133, 10.1007/s11027-006-9045-6, 2007.

Huffman, G. J., Bolvin, D. T., Nelkin, E. J., Wolff, D. B., Adler, R. F., Gu, G., Hong, Y., Bowman, K. P., and Stocker, E. F.: The TRMM Multisatellite Precipitation Analysis (TMPA): Quasi-Global, Multiyear, Combined-Sensor Precipitation Estimates at Fine Scales, Journal of Hydrometeorology, 8, 38-55, 10.1175/JHM560.1, 2007.

Johnston, F. H., Henderson, S. B., Chen, Y., Randerson, J. T., Marlier, M., Defries, R. S., Kinney, P., Bowman, D. M., and Brauer, M.: Estimated global mortality attributable to smoke from landscape fires Environ. Health Perspect. , 120 695–701, 2012.

Kim, D., Wang, C., Ekman, A. M. L., Barth, M. C., and Rasch, P. J.: Distribution and direct radiative forcing of carbonaceous and sulfate aerosols in an interactive

Atmos. Chem. Phys. Discuss., doi:10.5194/acp-2016-504, 2016
Manuscript under review for journal Atmos. Chem. Phys.
Published: 20 June 2016

size-resolving aerosol–climate model, Journal of Geophysical Research: Atmospheres, 113, D16309, 10.1029/2007jd009756, 2008.

Koe, L. C. C., Arellano Jr, A. F., and McGregor, J. L.: Investigating the haze transport from 1997 biomass burning in Southeast Asia: its impact upon Singapore, Atmospheric Environment, 35, 2723-2734, 2001.

Kunii, O., Kanagawa, S., Yajima, I., Hisamatsu, Y., Yamamura, S., Amagai, T., and Ismail, I. T. S.: The 1997 Haze Disaster in Indonesia: Its Air Quality and Health Effects, Archives of Environmental Health: An International Journal, 57, 16-22, 10.1080/00039890209602912, 2002.

Langner, A., Miettinen, J., and Siegert, F.: Land cover change 2002–2005 in Borneo and the role of fire derived from MODIS imagery, Global Change Biology, 13, 2329-2340, 10.1111/j.1365-2486.2007.01442.x, 2007.

Lin, N.-H., Tsay, S.-C., Maring, H. B., Yen, M.-C., Sheu, G.-R., Wang, S.-H., Chi, K. H., Chuang, M.-T., Ou-Yang, C.-F., Fu, J. S., Reid, J. S., Lee, C.-T., Wang, L.-C., Wang, J.-L., Hsu, C. N., Sayer, A. M., Holben, B. N., Chu, Y.-C., Nguyen, X. A., Sopajaree, K., Chen, S.-J., Cheng, M.-T., Tsuang, B.-J., Tsai, C.-J., Peng, C.-M., Schnell, R. C., Conway, T., Chang, C.-T., Lin, K.-S., Tsai, Y. I., Lee, W.-J., Chang, S.-C., Liu, J.-J., Chiang, W.-L., Huang, S.-J., Lin, T.-H., and Liu, G.-R.: An overview of regional experiments on biomass burning aerosols and related pollutants in Southeast Asia: From BASE-ASIA and the Dongsha Experiment to 7-SEAS, Atmospheric Environment, 78, 1-19, 2013.

Atmos. Chem. Phys. Discuss., doi:10.5194/acp-2016-504, 2016
Manuscript under review for journal Atmos. Chem. Phys.
Published: 20 June 2016

Madden, R. A., and Julian, P. R.: Detection of a 40–50 Day Oscillation in the Zonal Wind in the Tropical Pacific, Journal of the Atmospheric Sciences, 28, 702-708, 10.1175/1520-0469(1971)028<0702:DOADOI>2.0.CO;2, 1971.

Mauderly, J. L., and Chow, J. C.: Health effects of organic aerosols, Inhalation Toxicology, 20, 257-288, 2008.

Miriam, E. M., Ruth, S. D., Patrick, S. K., David, L. A. G., Shannon, N. K., Daniel, J. J., Loretta, J. M., Belinda, A. M., and Samuel, S. M.: Regional air quality impacts of future fire emissions in Sumatra and Kalimantan, Environmental Research Letters, 10, 054010, 2015a.

Miriam, E. M., Ruth, S. D., Patrick, S. K., Shannon, N. K., Daniel, J. J., Loretta, J. M., and Samuel, S. M.: Fire emissions and regional air quality impacts from fires in oil palm, timber, and logging concessions in Indonesia, Environmental Research Letters, 10, 085005, 2015b.

Page, S. E., Siegert, F., Rieley, J. O., Boehm, H.-D. V., Jaya, A., and Limin, S.: The amount of carbon released from peat and forest fires in Indonesia during 1997, Nature, 420, 61-65, 2002.

Randerson, J. T., Chen, Y., van der Werf, G. R., Rogers, B. M., and Morton, D. C.: Global burned area and biomass burning emissions from small fires, Journal of Geophysical Research: Biogeosciences, 117, G04012, 10.1029/2012JG002128, 2012.

Rasmusson, E. M., and Wallace, J. M.: Meteorological Aspects of the El Niño/Southern Oscillation, Science, 222, 1195-1202, 10.1126/science.222.4629.1195, 1983.

Reddington, C. L., Yoshioka, M., Balasubramanian, R., Ridley, D., Toh, Y. Y., Arnold, S. R., and Spracklen, D. V.: Contribution of vegetation and peat fires to particulate air pollution in Southeast Asia, Environmental Research Letters, 9, 094006, 2014.

Reid, J. S., Xian, P., Hyer, E. J., Flatau, M. K., Ramirez, E. M., Turk, F. J., Sampson, C. R., Zhang, C., Fukada, E. M., and Maloney, E. D.: Multi-scale meteorological conceptual analysis of observed active fire hotspot activity and smoke optical depth in the Maritime Continent, Atmos. Chem. Phys., 12, 2117-2147, 10.5194/acp-12-2117-2012, 2012.

Reid, J. S., Lagrosas, N. D., Jonsson, H. H., Reid, E. A., Sessions, W. R., Simpas, J. B., Uy, S. N., Boyd, T. J., Atwood, S. A., Blake, D. R., Campbell, J. R., Cliff, S. S., Holben, B. N., Holz, R. E., Hyer, E. J., Lynch, P., Meinardi, S., Posselt, D. J., Richardson, K. A., Salinas, S. V., Smirnov, A., Wang, Q., Yu, L., and Zhang, J.: Observations of the temporal variability in aerosol properties and their relationships to meteorology in the summer monsoonal South China Sea/East Sea: the scale-dependent role of monsoonal flows, the Madden–Julian Oscillation, tropical cyclones, squall lines and cold pools, Atmos. Chem. Phys., 15, 1745-1768, 10.5194/acp-15-1745-2015, 2015.

Saji, N. H., Goswami, B. N., Vinayachandran, P. N., and Yamagata, T.: A dipole mode in the tropical Indian Ocean, Nature, 401, 360-363, 1999.

See, S. W., Balasubramanian, R., and Wang, W.: A study of the physical, chemical, and optical properties of ambient aerosol particles in Southeast Asia during hazy and nonhazy days, Journal of Geophysical Research: Atmospheres, 111, D10S08, 10.1029/2005JD006180, 2006.

Atmos. Chem. Phys. Discuss., doi:10.5194/acp-2016-504, 2016
Manuscript under review for journal Atmos. Chem. Phys.
Published: 20 June 2016

Seinfeld, J., and Pandis, S.: Atmospheric Physics and Chemistry. From Air Pollution to Climate Change, Second Edition ed., New York (NY): JohnWiley & Sons, 2006.

Sekiguchi, M., Nakajima, T., Suzuki, K., Kawamoto, K., Higurashi, A., Rosenfeld, D., Sano, I., and Mukai, S.: A study of the direct and indirect effects of aerosols using global satellite data sets of aerosol and cloud parameters, Journal of Geophysical Research: Atmospheres, 108, 4699, 10.1029/2002JD003359, 2003.

Skamarock, W. C., Klemp, J. B., Dudhia, J., Gill, D. O., Barker, D. M., Duda, M. G., Huang, X.-Y., Wang, W., and Powers, J. G.: A Description of the Advanced Research WRF Version 3, NCAR Technical Note, NCAR/TN-475+STR, 2008.

Smith, A., Lott, N., and Vose, R.: The Integrated Surface Database: Recent Developments and Partnerships, Bulletin of the American Meteorological Society, 92, 704-708, doi:10.1175/2011BAMS3015.1, 2011.

Stauffer, D. R., and Seaman, N. L.: Multiscale Four-Dimensional Data Assimilation, Journal of Applied Meteorology, 33, 416-434, 10.1175/1520-0450(1994)033<0416:mfdda>2.0.co;2, 1994.

Tosca, M. G., Randerson, J. T., Zender, C. S., Flanner, M. G., and Rasch, P. J.: Do biomass burning aerosols intensify drought in equatorial Asia during El Niño?, Atmos. Chem. Phys., 10, 3515-3528, 10.5194/acp-10-3515-2010, 2010.

Tosca, M. G., Randerson, J. T., Zender, C. S., Nelson, D. L., Diner, D. J., and Logan, J. A.: Dynamics of fire plumes and smoke clouds associated with peat and deforestation fires in Indonesia, Journal of Geophysical Research: Atmospheres, 116, n/a-n/a, 10.1029/2010JD015148, 2011.

Atmos. Chem. Phys. Discuss., doi:10.5194/acp-2016-504, 2016
Manuscript under review for journal Atmos. Chem. Phys.
Published: 20 June 2016

Atmospheric Chemistry and Physics Discussions
Open Access

van der Werf, G. R., Randerson, J. T., Giglio, L., Collatz, G. J., Mu, M., Kasibhatla, P. S., Morton, D. C., DeFries, R. S., Jin, Y., and van Leeuwen, T. T.: Global fire emissions and the contribution of deforestation, savanna, forest, agricultural, and peat fires (1997–2009), Atmos. Chem. Phys., 10, 11707-11735, 10.5194/acp-10-11707-2010, 2010.

Wang, J., Ge, C., Yang, Z., Hyer, E. J., Reid, J. S., Chew, B.-N., Mahmud, M., Zhang, Y., and Zhang, M.: Mesoscale modeling of smoke transport over the Southeast Asian Maritime Continent: Interplay of sea breeze, trade wind, typhoon, and topography, Atmospheric Research, 122, 486-503, 2013.

Wiedinmyer, C., Akagi, S. K., Yokelson, R. J., Emmons, L. K., Al-Saadi, J. A., Orlando, J. J., and Soja, A. J.: The Fire INventory from NCAR (FINN): a high resolution global model to estimate the emissions from open burning, Geosci. Model Dev., 4, 625-641, 10.5194/gmd-4-625-2011, 2011.

Wu, C.-H., and Hsu, H.-H.: Topographic Influence on the MJO in the Maritime Continent, Journal of Climate, 22, 5433-5448, 10.1175/2009JCLI2825.1, 2009.

Wu, R., Wen, Z., and He, Z.: ENSO Contribution to Aerosol Variations over the Maritime Continent and the Western North Pacific during 2000–10, Journal of Climate, 26, 6541-6560, 10.1175/JCLI-D-12-00253.1, 2013.

Atmos. Chem. Phys. Discuss., doi:10.5194/acp-2016-504, 2016
Manuscript under review for journal Atmos. Chem. Phys.
Published: 20 June 2016

Atmospheric Chemistry and Physics Discussions

Table 1. WRF physics scheme configuration

Physics Processes	Scheme
microphysics	Morrison (2 moments) scheme
longwave radiation	rrtmg scheme
shortwave radiation	rrtmg scheme
surface-layer	MYNN surface layer
land surface	Unified Noah land-surface model
planetary boundary layer	MYNN 2.5 level TKE scheme
cumulus parameterization	Grell-Freitas ensemble scheme

Atmos. Chem. Phys. Discuss., doi:10.5194/acp-2016-504, 2016
Manuscript under review for journal Atmos. Chem. Phys.
Published: 20 June 2016

Table 2. Annual mean low visibility days (LVDs) and very low visibility days (VLVDs) per year, and the percentage contributions along with standard deviations of fire and non-fire (other) pollutions for total low visibility days in Bangkok, Kuala Lumpur, Singapore and Kuching during 2002-2014 (FNL_GFED is from 2003 to 2014). Parentheses show the percentage of year.

FNL_FINN	**LVD per year (days)**	**Fire pollution contribution (%)**	**Other pollution contribution (%)**
Bangkok, Thailand	211±49 (58±14%)	38±8	62±8
Kuala Lumpur, Malaysia	166±80 (45±22%)	35±18	65±18
Singapore, Singapore	92±84 (25±23%)	34±16	67±16
Kuching, Malaysia	95±54 (26±15%)	32±14	68±14
FNL_FINN	**VLVD per year (days)**	**Fire pollution contribution (%)**	**Other pollution contribution (%)**
Bangkok, Thailand	17±10 (5±3%)	89±19	11±19
Kuala Lumpur, Malaysia	18±18 (5±5%)	85±17	15±17
Singapore, Singapore	4±4 (1±1%)	92±32	8±32
Kuching, Malaysia	24±19 (7±5%)	94±12	6±12
ERA_FINN	**VLD per year (days)**	**Fire pollution contribution (%)**	**Other pollution contribution (%)**
Bangkok, Thailand	211±49 (58±14%)	45±8	55±8
Kuala Lumpur, Malaysia	166±80 (45±22%)	39±16	61±16
Singapore, Singapore	92±84 (25±23%)	37±18	63±18
Kuching, Malaysia	95±54 (26±15%)	44±17	56±17
ERA_FINN	**VLVD per year (days)**	**Fire pollution contribution (%)**	**Other pollution contribution (%)**
Bangkok, Thailand	17±10 (5±3%)	90±20	10±20
Kuala Lumpur, Malaysia	18±18 (5±5%)	90±18	10±18
Singapore, Singapore	4±4 (1±1%)	98±5	2±5
Kuching, Malaysia	24±19 (7±5%)	95±11	5±11
FNL_GFED	**VLD per year (days)**	**Fire pollution contribution (%)**	**Other pollution contribution (%)**
Bangkok, Thailand	215±50 (59±14%)	36±8	64±8
Kuala Lumpur, Malaysia	174±78 (48±21%)	28±17	72±17
Singapore, Singapore	96±87 (26±24%)	29±21	71±21
Kuching, Malaysia	95±57 (26±15%)	26±18	74±18
FNL_GFED	**VLVD per year (days)**	**Fire pollution contribution (%)**	**Other pollution contribution (%)**
Bangkok, Thailand	15±8 (4±2%)	90±19	10±19
Kuala Lumpur, Malaysia	18±18 (5±5%)	83±28	17±28
Singapore, Singapore	4±4 (1±1%)	89±37	11±37
Kuching, Malaysia	22±18 (6±5%)	89±28	11±28

Atmos. Chem. Phys. Discuss., doi:10.5194/acp-2016-504, 2016
Manuscript under review for journal Atmos. Chem. Phys.
Published: 20 June 2016

Atmospheric Chemistry and Physics Discussions
Open Access
EGU

Table 3. Annual mean and standard deviation of fire $PM_{2.5}$ concentration (μg m^{-3}) contributed by each source region in Bangkok, Kuala Lumpur, Singapore, and Kuching during 2002-2014 (FNL_GFED is from 2003 to 2014). Parentheses show the fire aerosol fraction in total $PM_{2.5}$.

FNL_FINN	**s1**	**s2**	**s3**	**s4**	**s5**
Bangkok	8.0±2.6 (99.1±0.5%)	0.0±0.0 (0.1±0.1%)	0.0±0.0 (0.1±0.1%)	0.0±0.0 (0.7±0.5%)	0.0±0.0 (0.0±0.0%)
Kuala Lumpur	2.1±1.2 (43.3±14.6%)	2.5±1.4 (49.3±14.3%)	0.2±0.1 (4.1±4.4%)	0.1±0.1 (2.9±2.6%)	0.0±0.0 (0.4±0.2%)
Singapore	1.0±0.7 (34.3±16.4%)	1.2±0.8 (40.7±15.3%)	0.5±0.4 (16.0±11.3%)	0.2±0.1 (6.7±4.2%)	0.1±0.0 (2.2±1.1%)
Kuching	0.4±0.4 (7.3±6.6%)	0.3±0.1 (4.6±2.4%)	6.3±3.2 (85.3±9.6%)	0.1±0.1 (2.3±2.3%)	0.0±0.0 (0.6±0.2%)
ERA_FINN	**s1**	**s2**	**s3**	**s4**	**s5**
Bangkok	8.7±2.7 (99.1±0.4%)	0.0±0.0 (0.1±0.1%)	0.0±0.0 (0.1±0.1%)	0.1±0.0 (0.7±0.4%)	0.0±0.0 (0.0±0.0%)
Kuala Lumpur	2.1±1.2 (38.6±12.7%)	3.0±1.5 (53.7±11.9%)	0.2±0.2 (4.7±4.2%)	0.1±0.0 (2.6±2.1%)	0.0±0.0 (0.4±0.2%)
Singapore	1.0±0.6 (31.9±15.3%)	1.4±0.9 (40.4±13.1%)	0.7±0.6 (18.9±12.8%)	0.2±0.1 (6.8±3.7%)	0.1±0.0 (1.9±1.0%)
Kuching	0.5±0.4 (7.5±5.7%)	0.4±0.2 (5.9±3.9%)	6.9±3.8 (83.4±10.1%)	0.1±0.1 (2.7±2.9%)	0.0±0.0 (0.6±0.2%)
FNL_GFED	**s1**	**s2**	**s3**	**s4**	**s5**
Bangkok	4.8±1.3 (99.6±0.2%)	0.0±0.0 (0.1±0.0%)	0.0±0.0 (0.1±0.1%)	0.0±0.0 (0.2±0.2%)	0.0±0.0 (0.1±0.0%)
Kuala Lumpur	1.3±0.6 (38.6±20.8%)	2.7±1.9 (53.8±21.1%)	0.1±0.2 (2.8±3.5%)	0.0±0.0 (0.8±0.8%)	0.1±0.1 (3.9±3.4%)
Singapore	0.3±0.2 (22.1±17.3%)	1.5±1.8 (40.2±23.6%)	0.4±0.5 (12.5±9.5%)	0.1±0.0 (2.9±2.4%)	0.4±0.2 (22.3±13.2%)
Kuching	0.1±0.1 (7.2±6.8%)	0.1±0.1 (4.3±3.2%)	3.2±3.2 (75.2±12.9%)	0.0±0.0 (1.7±2.7%)	0.3±0.2 (11.6±6.7%)

Atmos. Chem. Phys. Discuss., doi:10.5194/acp-2016-504, 2016
Manuscript under review for journal Atmos. Chem. Phys.
Published: 20 June 2016

Atmospheric Chemistry and Physics Discussions
Open Access

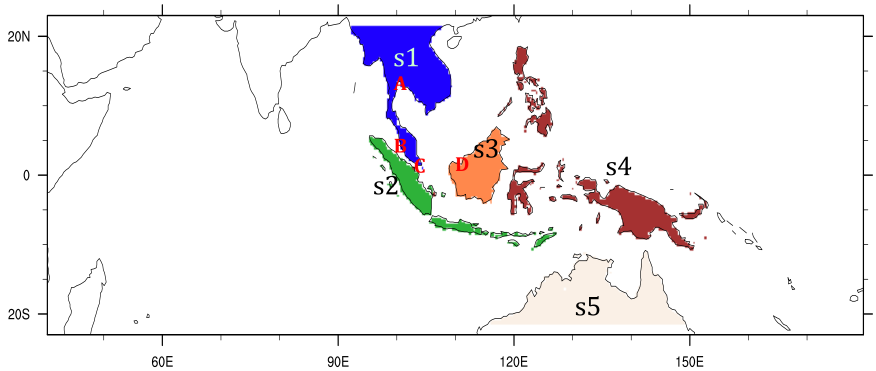

Figure 1. Model domain used for simulations. Domain consists of 31 vertical levels, each with 432 × 148 grid points with a horizontal resolution of 36 km. Five colored fire source regions, labeled as s1, s2, s3, s4 and s5, represent Mainland Southeast Asia, Sumatra and Java islands, Borneo, the rest of Maritime Continent, and northern Australia, respectively. A, B, C and D indicate the location of four selected cities: Bangkok, Kuala Lumpur, Singapore and Kuching, respectively.

Atmos. Chem. Phys. Discuss., doi:10.5194/acp-2016-504, 2016
Manuscript under review for journal Atmos. Chem. Phys.
Published: 20 June 2016

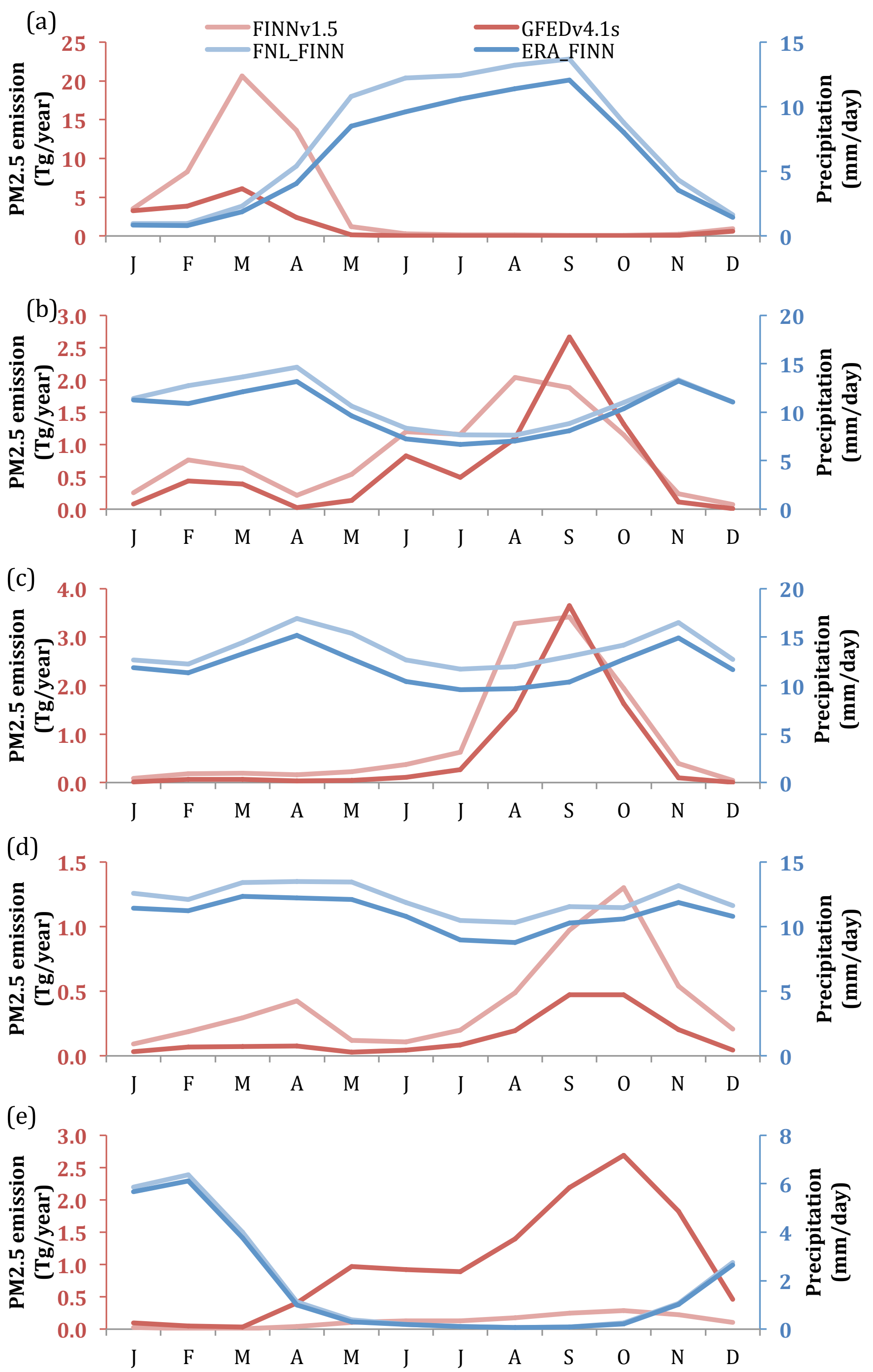

Atmos. Chem. Phys. Discuss., doi:10.5194/acp-2016-504, 2016
Manuscript under review for journal Atmos. Chem. Phys.
Published: 20 June 2016

Figure 2. Monthly $PM_{2.5}$ emissions (Tg year^{-1}) in FINNv1.5 (red lines) and GFEDv4.1s (pink lines). Also shown are precipitation rate (mm day^{-1}) simulated in FNL_FINN (light blue lines) and ERA_FINN (blue lines). All data are averaged during 2002-2014 for: (a) Mainland Southeast Asia (s1), (b) Sumatra and Java islands (s2), (c) Borneo (s3), (d) the rest of the Maritime Continent (s4), and (e) northern Australia (s5). Note that GFEDv4.1s $PM_{2.5}$ emission is averaged from 2003 to 2014.

Atmos. Chem. Phys. Discuss., doi:10.5194/acp-2016-504, 2016
Manuscript under review for journal Atmos. Chem. Phys.
Published: 20 June 2016

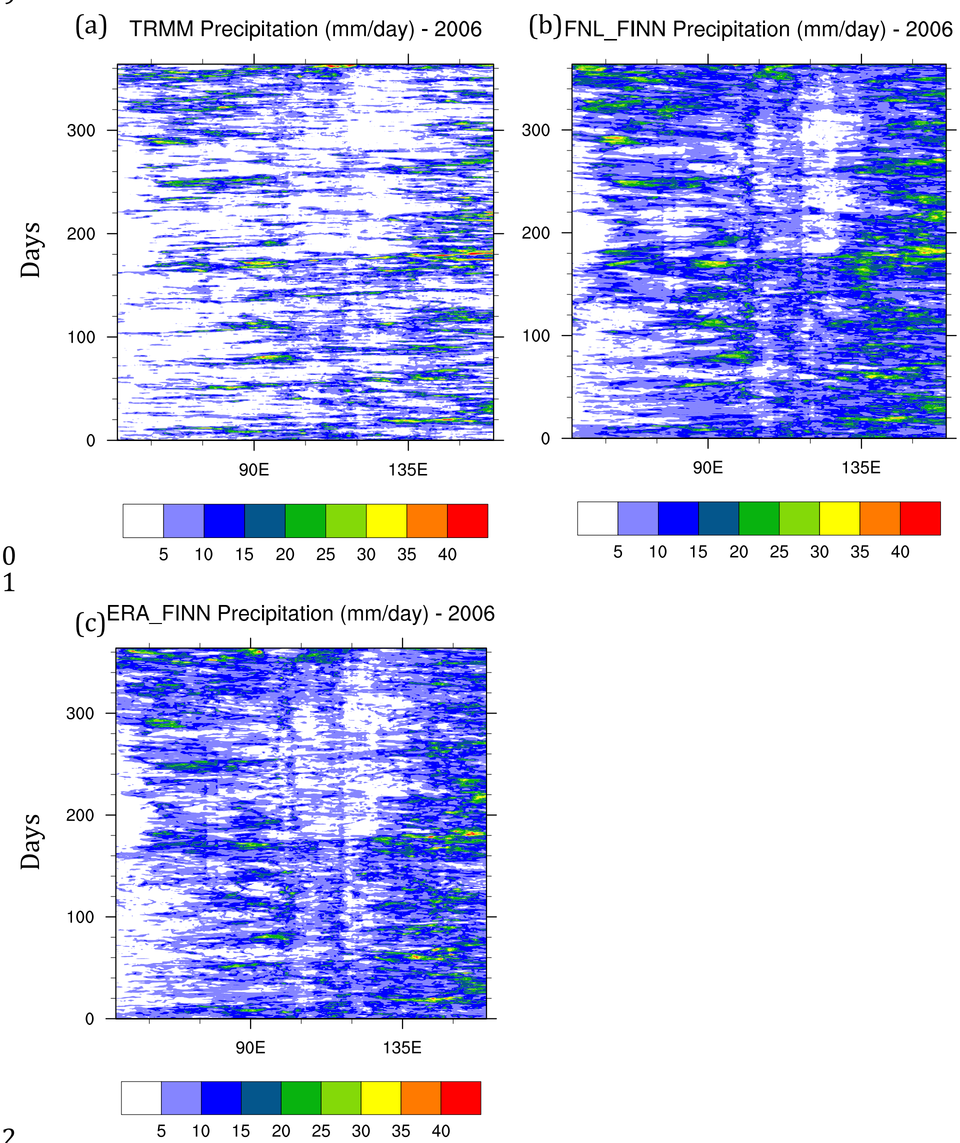

Figure 3. Hovmöller (time vs. longitude) plot of daily precipitation in 2006 derived from: (a) TRMM, (b) FNL_FINN, and (c) ERA_FINN. Latitude average is from 10°S to 10°N. Unit is mm day^{-1}.

Atmos. Chem. Phys. Discuss., doi:10.5194/acp-2016-504, 2016
Manuscript under review for journal Atmos. Chem. Phys.
Published: 20 June 2016

Atmospheric Chemistry and Physics
Discussions
Open Access

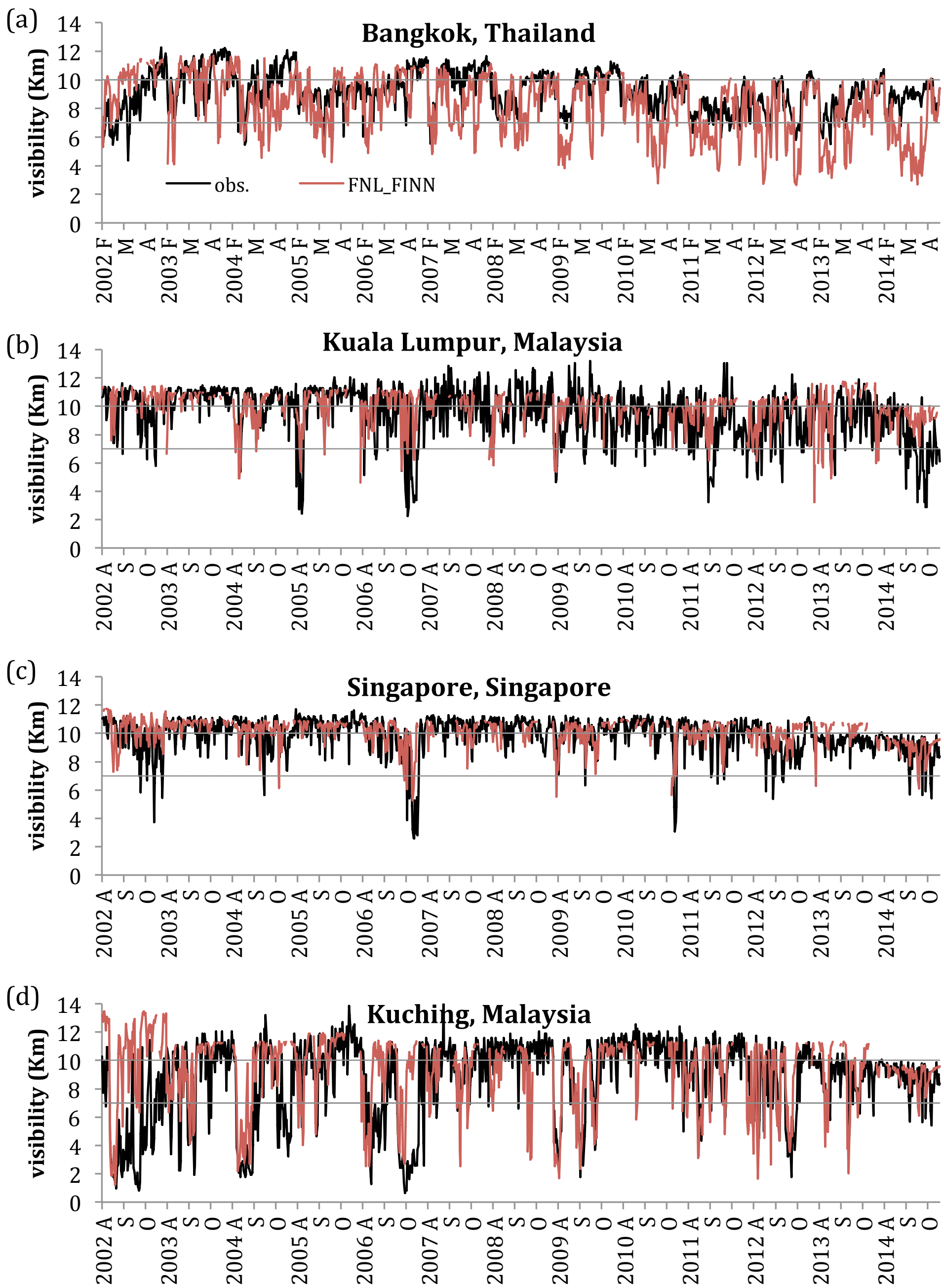

Figure 4. Comparison of daily visibility between GSOD observation (black lines) and FNL_FINN modeled result (red lines) in: (a) Bangkok, (b) Kuala Lumpur, (c) Singapore, (d) Kuching during the fire seasons from 2002 to 2014. Two grey lines mark the visibility of 7 and 10 km, respectively.

Atmos. Chem. Phys. Discuss., doi:10.5194/acp-2016-504, 2016
Manuscript under review for journal Atmos. Chem. Phys.
Published: 20 June 2016

Atmospheric Chemistry and Physics
Discussions
Open Access

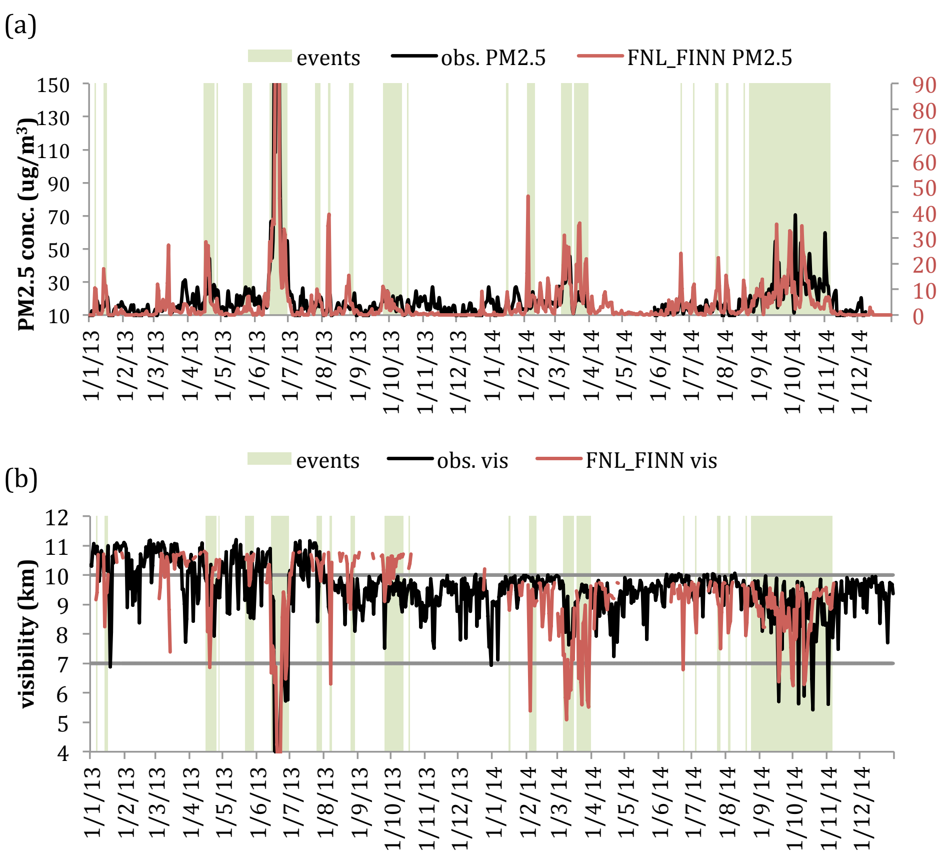

Figure 5. (a) Time series of daily surface $PM_{2.5}$ from the ground-based observations (black line) and FNL_FINN simulated results (red line) in Singapore during 2013-2014. (b) Time series of daily visibility of GSOD observation (black line) and calculated result from FNL_FINN (red line) in Singapore during 2013-2014. Highlighted green areas are known haze events caused by fire aerosols. Two gray lines mark the visibility of 7 and 10 km, respectively.

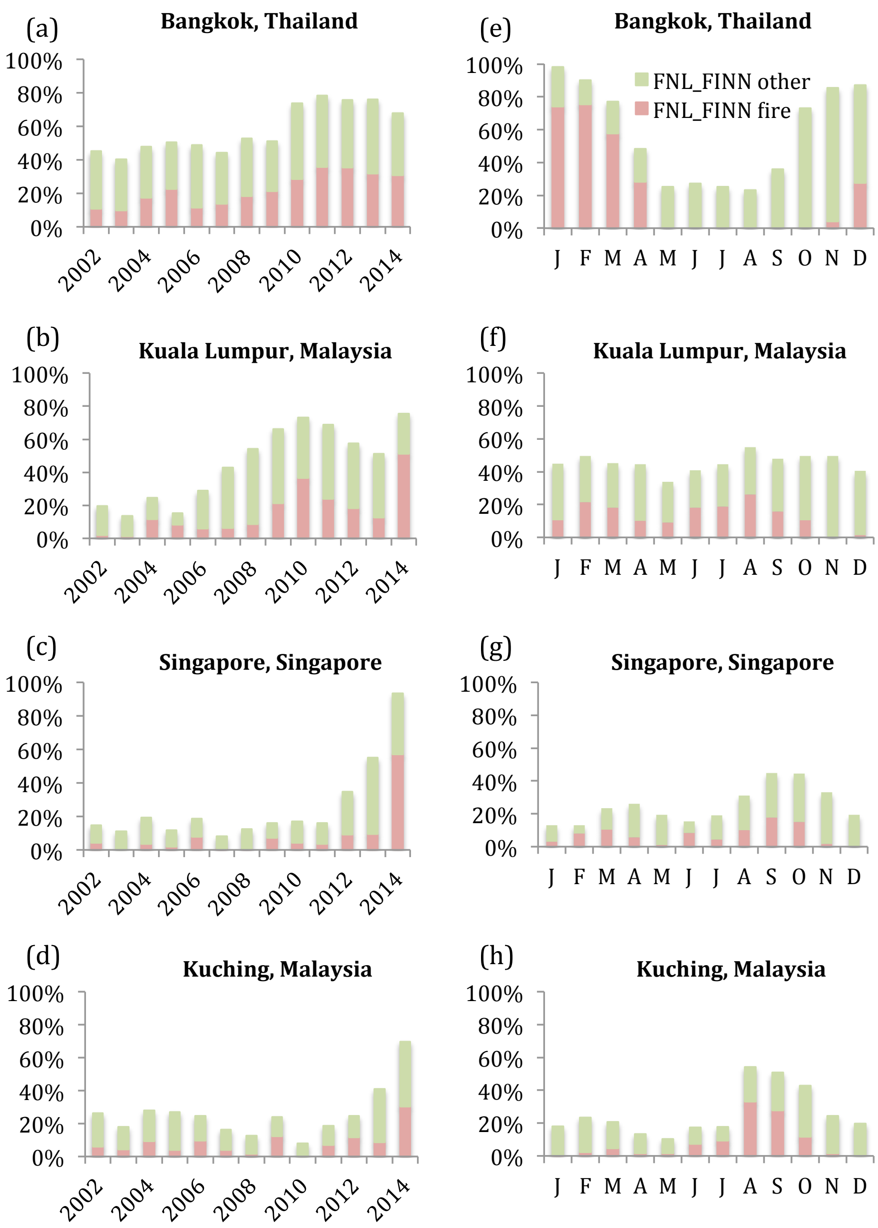

Figure 6. (a) – (d) The annual variation of the percentage of LVDs per year from GSOD observational visibility in Bangkok, Kuala Lumpur, Singapore, and Kuching, respectively. (e) – (h) The monthly variation of the percentage of LVDs from GSOD observational visibility in Bangkok, Kuala Lumpur, Singapore, and Kuching, respectively, averaged over 2002-2014.

Atmos. Chem. Phys. Discuss., doi:10.5194/acp-2016-504, 2016
Manuscript under review for journal Atmos. Chem. Phys.
Published: 20 June 2016

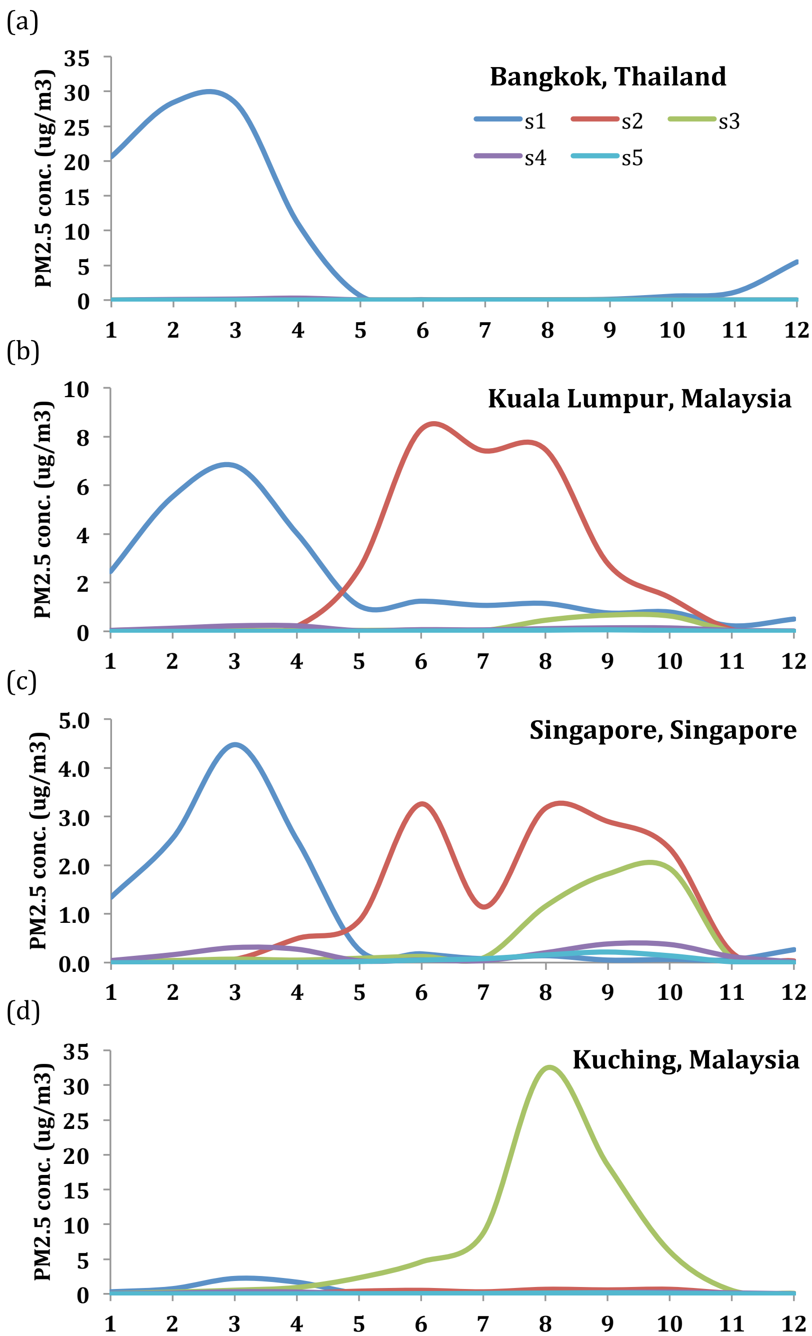

Figure 7. The monthly variation of mean $PM_{2.5}$ concentration from each emission regions (s1 - s5) in (a) Bangkok, (b) Kuala Lumpur, (c) Singapore and (d) Kuching, derived from FNL_FINN simulation and averaged over the period 2002-2014.

Atmos. Chem. Phys. Discuss., doi:10.5194/acp-2016-504, 2016
Manuscript under review for journal Atmos. Chem. Phys.
Published: 20 June 2016

Atmospheric Chemistry and Physics
Discussions

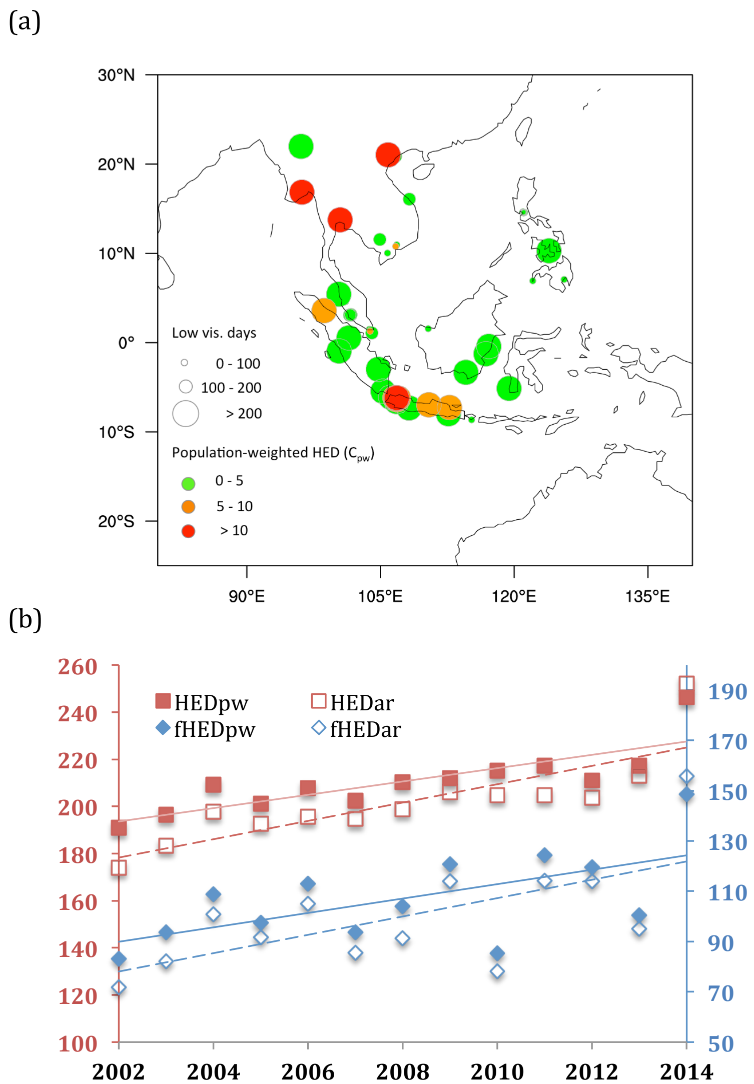

Figure 8. (a) The mean low visibility days (circles) per year from 2002 to 2014 in 50 ASEAN cities and their population-weighted fraction in the total Haze Exposure Days (HED; colors). (b) Annual variation of population-weighted HED (HED_{pw}) and arithmetic mean HED (HED_{ar}). Fire-caused HED are labeled as $fHED_{pw}$ and $fHED_{ar}$. Units are in days.

Atmos. Chem. Phys. Discuss., doi:10.5194/acp-2016-504, 2016
Manuscript under review for journal Atmos. Chem. Phys.
Published: 20 June 2016

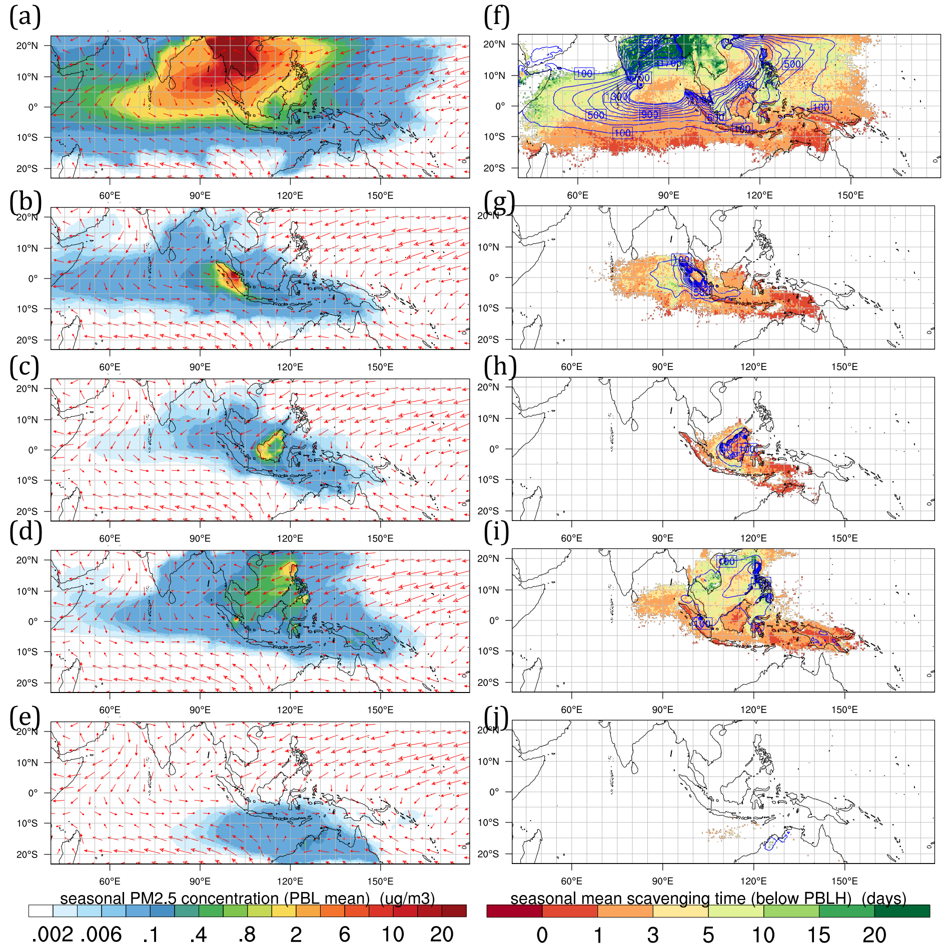

Figure 9. (a)-(e) Seasonal mean $PM_{2.5}$ concentration (μg m^{-3}) and wind within the PBL modeled in FNL_FINN during February to April, 2002 – 2014 in: Mainland Southeast Asia (s1), Sumatra and Java island (s2), Borneo (s3), the rest of the Maritime Continent (s4), and northern Australia (s5), respectively. (f)-(g) Same as (a)-(e) but for seasonal mean wet scavenging time (days; shaded) and column intergraded $PM_{2.5}$ concentration (μg m^{-2}; contours) within the PBL height.

Atmos. Chem. Phys. Discuss., doi:10.5194/acp-2016-504, 2016
Manuscript under review for journal Atmos. Chem. Phys.
Published: 20 June 2016

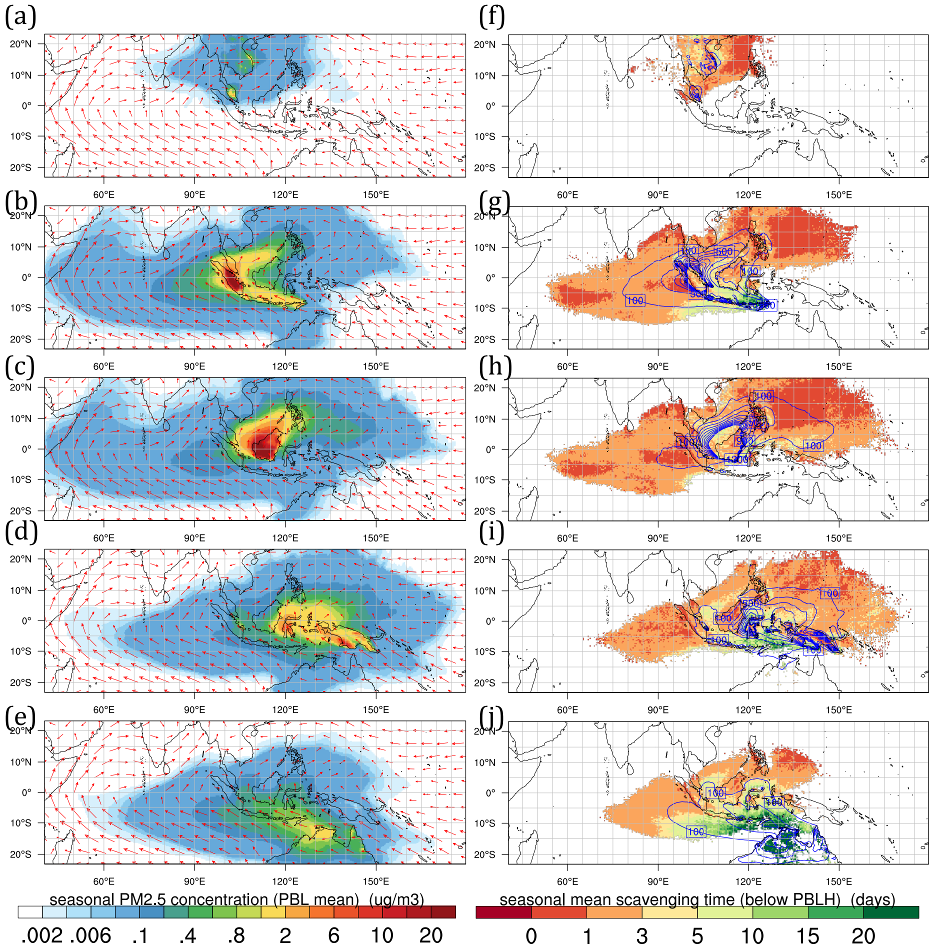

Figure 10. Same as Fig. 9 but during August to October, 2002 – 2014.

Atmos. Chem. Phys. Discuss., doi:10.5194/acp-2016-504, 2016
Manuscript under review for journal Atmos. Chem. Phys.
Published: 20 June 2016

Atmospheric Chemistry and Physics
Open Access
Discussions

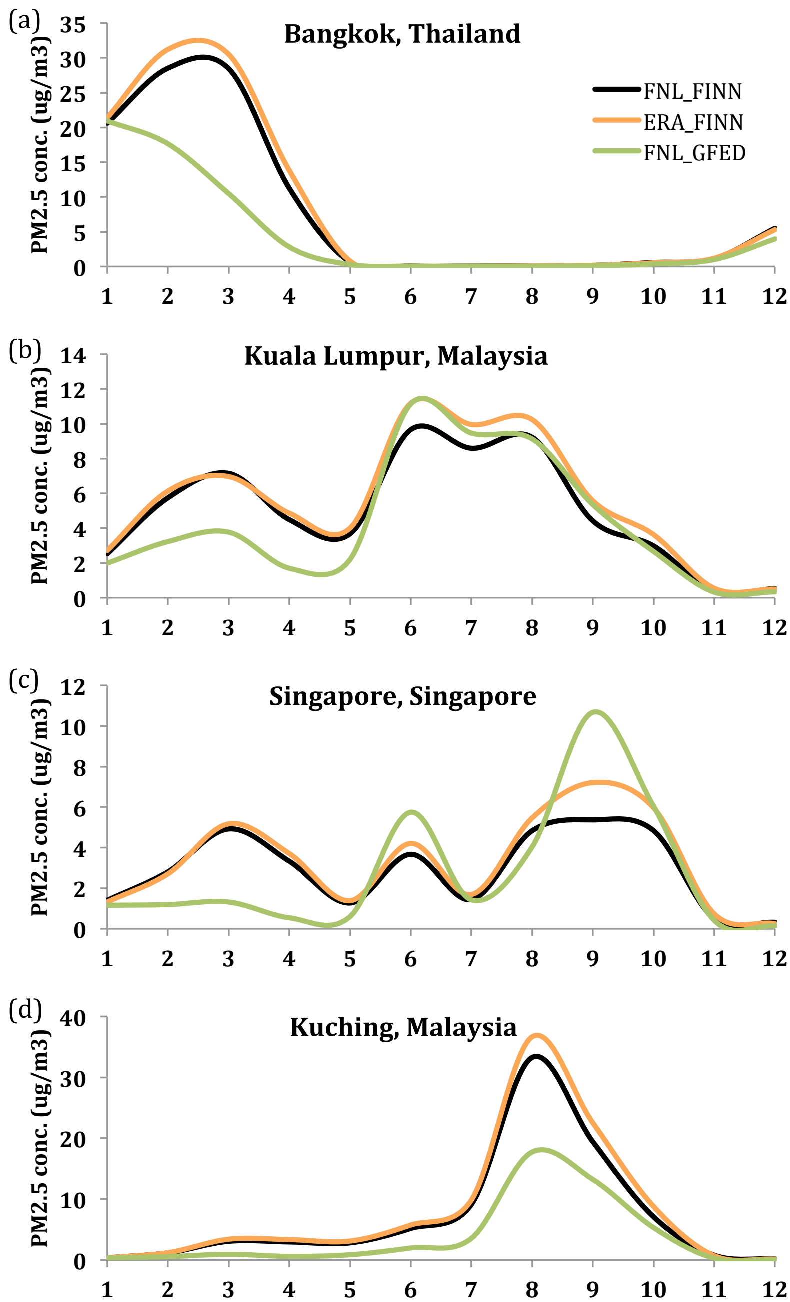

Figure 11. The monthly variation of mean $PM_{2.5}$ concentration in FNL_FINN, ERA_FINN, and FNL_GFED in: (a) Bangkok, (b) Kuala Lumpur, (c) Singapore, and (d) Kuching over the period 2002-2014 (FNL_GFED is from 2003 to 2014).

Atmos. Chem. Phys. Discuss., doi:10.5194/acp-2016-504, 2016
Manuscript under review for journal Atmos. Chem. Phys.
Published: 20 June 2016

Atmospheric Chemistry and Physics
Discussions
Open Access

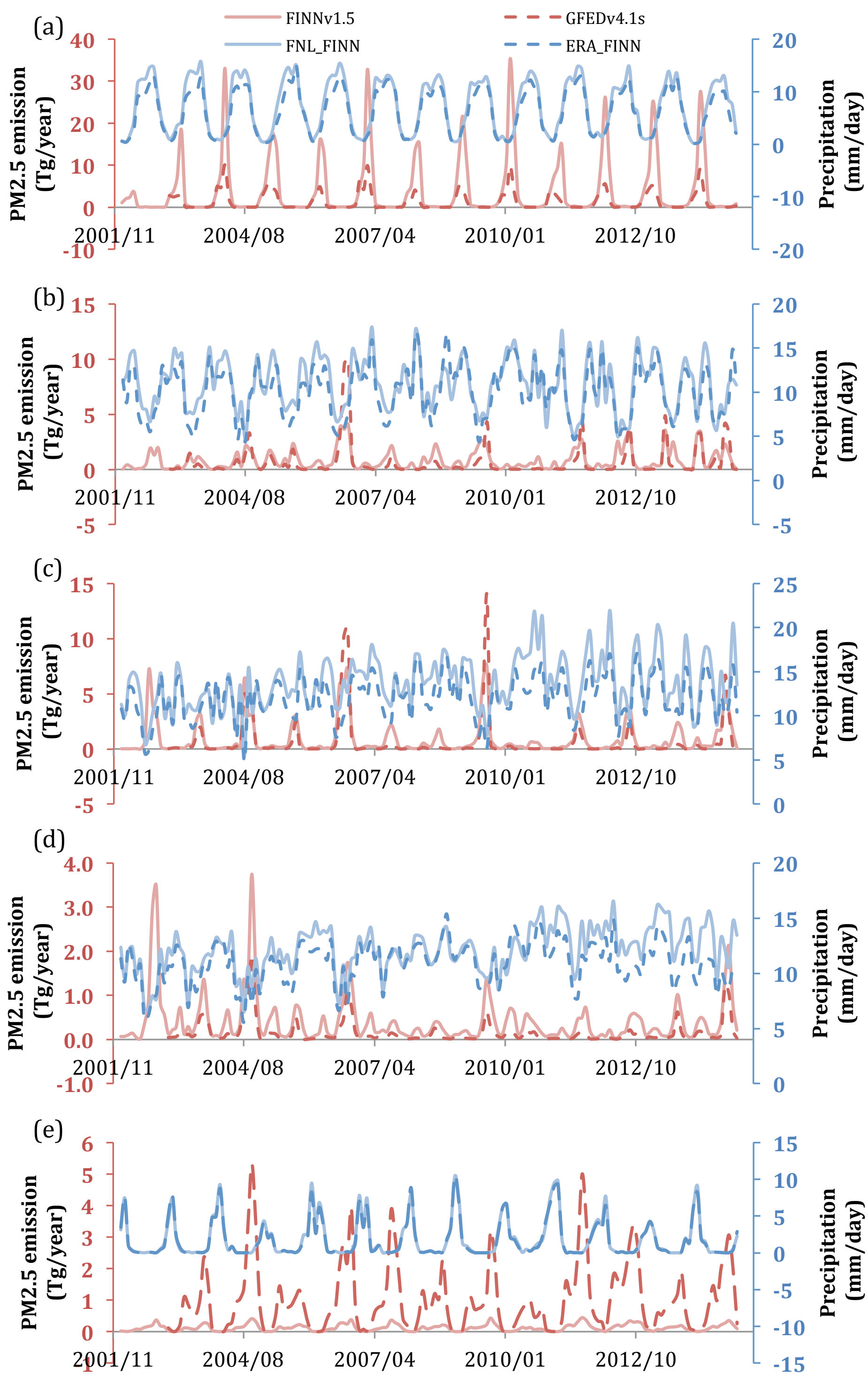

Atmos. Chem. Phys. Discuss., doi:10.5194/acp-2016-504, 2016
Manuscript under review for journal Atmos. Chem. Phys.
Published: 20 June 2016

Figure 12. Temporal variation of monthly $PM_{2.5}$ emission (Tg year^{-1}) in FINNv1.5 (pink solid lines) and GFEDv4.1s (red dashed lines). Also shown are precipitation rates (mm day^{-1}) simulated in FNL_FINN (light blue solid lines) and ERA_FINN (blue dashed lines) during 2002-2014 in: (a) Mainland Southeast Asia (s1), (b) Sumatra (s2), (c) Borneo (s3), (d) the rest of the Maritime Continent (s4), and (e) northern Australia (s5).

Atmos. Chem. Phys. Discuss., doi:10.5194/acp-2016-504, 2016
Manuscript under review for journal Atmos. Chem. Phys.
Published: 20 June 2016

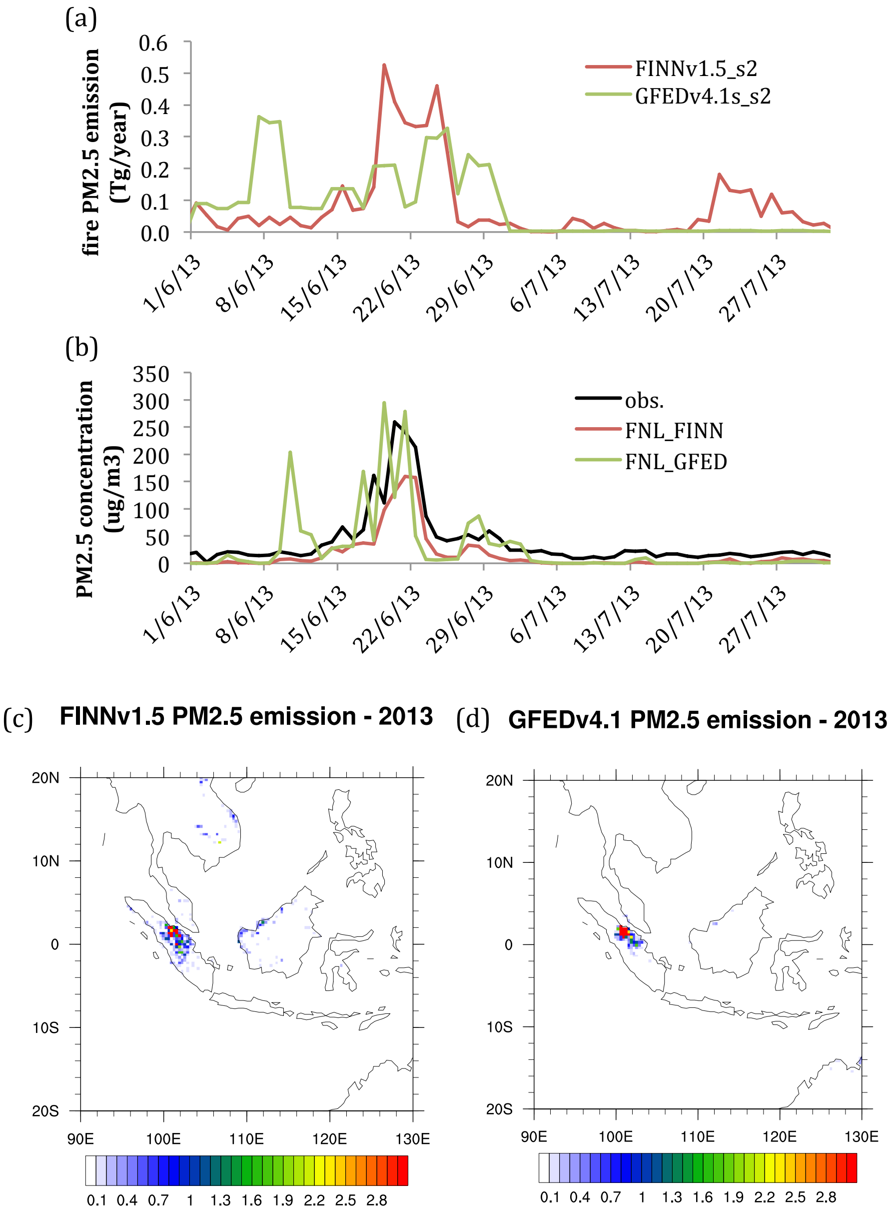

Figure 13. (a) Time series of daily mean $PM_{2.5}$ emissions (Tg year^{-1}) in Sumatra (s2) from FINNv1.5 (red line) and GFEDv4.1s (green line). (b) Time series of daily mean $PM_{2.5}$ concentration (μg m^{-3}) in Singapore from observation (black line), and modeled results from FNL_FINN (red line) and FNL_GFED (green line). (c) Monthly mean $PM_{2.5}$ emissions (Tg year^{-1}) from FINNv1.5 in June 2013. (d) same as (c) but from GFEDv4.1s.